DOI: https://doi.org/10.20870/oeno-one.2026.60.2.9663

OPEN ACCESS

VITICULTURE ORIGINAL RESEARCH ARTICLES

Oceanic viticulture across contrasting ENSO phases: A three-year field case study with Albariño and Tannat

Ramiro Tachini[1,2,*], Diego Piccardo[1], Hervé Quénol[2], Mercedes Fourment[1]

[1] Facultad de Agronomía, Universidad de la República Oriental del Uruguay. Av. Garzón 780, CP 12900 Montevideo, Uruguay

[2] Université Rennes 2, LETG-UMR 6554 CNRS, 2 Place Recteur Le Moal, 35 043 Rennes Cedex, France

Article number: 9663

**correspondence:*
rtachini@fagro.edu.uy

Associate editor:
João Santos

Received:
03 October 2025

Accepted:
07 April 2026

Published:
11 May 2026

This article is published under the **Creative Commons licence** (CC BY 4.0).

Use of all or part of the content of this article must mention the authors, the year of publication, the title, the name of the journal, the volume, the pages and the DOI in compliance with the information given above.

ABSTRACT

Climate change is expected to significantly alter the suitability of winegrowing regions, with direct consequences for grape yield and wine quality. Among the most widely studied adaptation strategies is the relocation of vineyards to cooler sites. In this context, a three-year field study was conducted to evaluate the physiological, agronomic, and metabolic responses of *Vitis vinifera* L. cvs. Albariño and Tannat across three sites located at the same latitude in southern Uruguay, but differing in topography and proximity to the Atlantic Ocean. The study spanned three growing seasons with contrasting ENSO phases: 2023 (La Niña, with the warmest summer in 50 years), 2024 (El Niño, characterised by temperate and humid conditions), and 2025 (Neutral). Albariño exhibited great stability across sites and vintages; however, oceanic plots consistently showed higher levels of titratable acidity, primarily due to malic acid, which impacted the soluble solids/acidity ratio. This situation occurred despite the fact that harvest dates were systematically later in oceanic areas, with a difference of up to 20 days. This condition favours slow ripening, which is desirable for aroma synthesis. Tannat displayed greater sensitivity to interannual climatic variation and site effects. Notably, within the oceanic plots, the more ocean-exposed site preserved higher malic acid levels, whereas the less exposed site showed higher anthocyanin concentrations. The 2023 growing season led to elevated leaf temperatures and vapour pressure deficits in both varieties, impacting net CO_2 assimilation, especially at the traditional inland site. The thermal pressure on both cultivars was associated with earlier harvest, particularly at the inland reference, where Tannat, in particular, showed a decrease in anthocyanins, indicating an imbalance in phenolic/technological ripening. Overall, oceanic conditions moderated thermal stress and reduced interannual variability, highlighting the buffering role of Atlantic influence under warm seasons. These findings suggest cultivar-specific interpretations: Albariño appears comparatively resilient under variable seasons, whereas Tannat may require site- and season-tailored management to maintain the balance between technological and phenolic maturity under warming conditions.

KEYWORDS: climate change adaptation, oceanic influence, viticulture, Albariño, Tannat, grape composition

INTRODUCTION

Grape production covers approximately 7 million hectares worldwide (OIV, 2024), making it one of the most important perennial fruit crops. The development and quality of grape production are closely linked to the climatic conditions of the cultivation site and are generally restricted to temperate zones, between latitudes 30° and 50° N and 30° and 40° S (Schultz & Jones, 2010).

The climate of a winegrowing region is determined by the interaction of multiple geographic and environmental factors, including latitude, altitude, continentality, and topography (Neethling *et al.*, 2019; Quénol, 2014). When these climatic variables are combined with soil characteristics, plant material, and vineyard management practices, the concept of terroir emerges (Deloire *et al.*, 2005). This term encompasses the unique combination of conditions in a specific location that impart distinctive qualities to the final wine. In wine-producing countries, the study and delineation of terroirs has a long-standing tradition and continues today with increasing precision. Concurrently, these terroirs are being subjected to climatic and agroclimatic modelling to project future scenarios (Le Roux *et al.*, 2017; Quénol, 2014), enabling proactive adaptation to climate change by identifying optimal plant-soil-climate combinations both now and in the future.

Uruguay, in South America, is considered part of the "New World" of viticulture. Today, viticulture is concentrated in the south-central region of the country (80 % of the planted area) (INAVI, 2025), near the capital city, Montevideo, directly linked to historical migration patterns. However, the search for new terroirs that provide unique wine typicity has led to the expansion of viticulture into new areas, particularly along the Atlantic coast. In the last 10 years, this oceanic region has expanded its vineyard surface by 65 % (INAVI, 2025). Both the traditional and Atlantic viticultural regions lie near 34° S and are classified as coastal areas under the Köppen climate classification "Cfa" (humid subtropical climate with hot summers and no dry season). The traditional inland region is 150 km away from the Atlantic Ocean and is located near the Río de la Plata estuary, with sea breezes influencing the viticulture region (Fourment *et al.*, 2014; Fourment *et al.*, 2017). However, significant differences exist in the oceanic influence of the Atlantic wine region. The Atlantic region experiences more direct oceanic exposure, resulting in a relatively cooler summer climate, especially in terms of maximum temperatures (INUMET, 2020). The situation is becoming more complex by the addition of topography, since the oceanic region has hills that vary the exposure to the ocean, modifying the mesoclimate (Tachini *et al.*, 2023).

Cooler summer conditions are increasingly considered advantageous for adapting viticulture to climate change and rising global temperatures. Common adaptation strategies include shifting vineyards to higher latitudes or altitudes (van Leeuwen *et al.*, 2024; Gutiérrez-Gamboa & Fourment, 2024). In Uruguay, the mean annual temperature has increased by approximately 2 °C over the past 50 years, and projections suggest an additional 2 to 4 °C rise by 2050, alongside more frequent and intense extreme events, such as heatwaves (IPCC, 2021). Given the country's limited altitudinal and latitudinal variability, the moderating effect of the Atlantic Ocean becomes a key factor for climate adaptation. This buffering capacity makes coastal areas strategic terroirs for implementing climate adaptation strategies (Fourment *et al.*, 2024; Tachini *et al.*, 2023). Additionally, Uruguay's climate is strongly influenced by interannual variability associated with the ENSO (El Niño-Southern Oscillation). La Niña phases are typically characterised by warm and dry conditions, while El Niño phases bring cooler and wetter conditions (Cai *et al.*, 2020). This variability amplifies the so-called vintage effect, which may negatively impact wine quality, consistency, and market value.

Among climatic factors, temperature and water availability are critical for grapevine cultivation and represent significant threats to viticultural sustainability under climate change (van Leeuwen *et al.*, 2024). Rising temperatures can severely impact vineyard productivity, with potential yield losses of up to 35 % in some regions due to heat stress (Fourment & Piccardo, 2023; Fraga, 2020). Summers exceeding 30 °C can accelerate grapevine phenology (Mira De Orduña, 2010), leading to rapid berry ripening during the hottest period of the season. This may result in lower anthocyanin and aroma compound accumulation, excessive sugar content, loss of acidity and unbalanced wines (Pons *et al.*, 2017; Sadras *et al.*, 2013).

In detail, the optimal temperature range for grapevine photosynthesis is between 25 °C and 35 °C. Above 35 °C, photosynthetic activity declines significantly due to stomatal closure, with irreversible damage occurring beyond 40 °C (Greer & Weston, 2010; Hochberg *et al.*, 2015; Torregrosa *et al.*, 2017). Heat stress also has a direct impact on berry quality. Sugar accumulation is most efficient between 20 °C and 30 °C, declining above 35 °C (Greer & Weston, 2010). Malic acid degrades above 25 °C and more significantly at higher temperatures (Brandt *et al.*, 2019). Anthocyanin biosynthesis is optimal around 30 °C but is affected above 35 °C (Mori *et al.*, 2007). Warm conditions initially reduce herbaceous notes of aroma compounds, especially methoxypyrazines. However, most desirable molecules are synthesised at the end of ripening, and their accumulation is enhanced by cooler conditions that slow maturation (Alem *et al.*, 2019; Pons *et al.*, 2017). Therefore, terroir-oriented studies should prioritise cultivars and sites with balanced proportions of tartaric and malic acid, low sugar content and high levels of acidity and anthocyanins, as key traits for sustainable viticulture in the context of climate change (Gutiérrez-Gamboa *et al.*, 2021; van Leeuwen *et al.*, 2019).

Tannat is the most widely planted variety in Uruguay, accounting for 27 % of vineyard area (INAVI, 2025). Native to the Atlantic Pyrenees, it is the most extensively studied variety in Uruguay (Ferrer *et al.*, 2020). Its popularity is due to its good adaptation to the Uruguayan environment, typicity, and high oenological potential, reflected in

elevated anthocyanin, tannin, and acidity levels (González-Neves *et al.*, 2010). Albariño, originally from Portugal, is a white variety introduced to Uruguay in the early 2000s from Galicia, Spain. Its vineyard surface in Uruguay has increased by 250 % over the past decade (INAVI, 2025). It is used for monovarietal wines of preferred quality (VCP) and is recognised for producing fresh, balanced wines with floral, fruity, and herbaceous aromas in its native region (Diéguez *et al.*, 2003; Vilanova & Vilariño, 2006). Most studies on Albariño's physiology and berry quality have been conducted in Europe, while in Uruguay, Fourment *et al*. (2024) have emphasised its high plasticity to adapt to the climatic variability of the oceanic terroir.

Accordingly, this study aims to characterise Tannat and Albariño varieties across two oceanic sites and compare them with a vineyard in the traditional inland region, over three climatically distinct growing seasons, with a particular emphasis on the 2022–2023 cycle, which was the warmest and driest growing season in the last 50 years. Specific objective was to: (1) quantify the effects of growing seasons, oceanic sites and their interaction on key physiological traits, yield components and berry metabolite profiles; (2) whether Albariño and Tannat differ in sensitivity to seasonal climatic conditions under oceanic environments; and (3) discuss the potential of oceanic vineyard conditions to buffer climate extremes relevant to cultivar performance in a warming context.

MATERIALS AND METHODS

1. Site characterisation and identification of plots under evaluation

Two winegrowing regions at 34° S were selected. The traditional inland region in southern Uruguay (Canelones; C), approximately 25 km from the Río de la Plata estuary. The oceanic region was located in eastern Uruguay (O), ~150 km East of Canelones and ~18 km from the Atlantic Ocean, in an emerging winegrowing area (Figure 1A).

The oceanic emerging wine region is an area of low hills with altitudes up to 150 m.a.s.l. The soils are Argiudoll (sand 51 %, silt 24 %, and clay 25 %), with a water-holding capacity of 18 mm/10 cm and slopes up to 20 % (Silva *et al.*, 2018). The main factor generating variability in plant response and grape composition is altitude in combination with ocean exposure (Tachini *et al.*, 2023). The traditional inland region is topographically flat with altitudes below 80 m.a.s.l and slopes between 1 and 2.2 %. The soils correspond to Hapludert (sand 15 %, silt 49 %, and clay 36 %) and a water-holding capacity of 21 mm/10 cm. In this region, meso-climatic variability is attributed to the distance from the La Plata River (Silva *et al.*, 2018; Fourment *et al.*, 2017).

Both vineyards (oceanic and inland) are managed with the objective of producing medium- to high-quality wines. The training system used is the Vertical Shoot Positioning system (VSP) with a long Guyot pruning system. The planting spacing is 2 × 1 in the oceanic region and 2.5 × 1 in the traditional region. In Albariño, no leaf removal is performed in any of the plots, and in the traditional inland region, crop load is regulated through post-veraison cluster thinning. For Tannat, leaf removal is conducted on one side of the canopy at both regions, and crop load is regulated through post-veraison cluster thinning. In both vineyards, inter-row spaces are covered with a spontaneous natural groundcover, while the vine rows are kept weed-free through herbicide applications. The harvest was determined by the pH level, with values between 3.10 and 3.20 stipulated for Albariño and between 3.20 and 3.30 for Tannat.

2. Vine measurements

A total of 12 productive vineyard plots of *Vitis vinifera* L. cv. Albariño and Tannat were selected in the oceanic region. These were classified into two groups based on elevation and

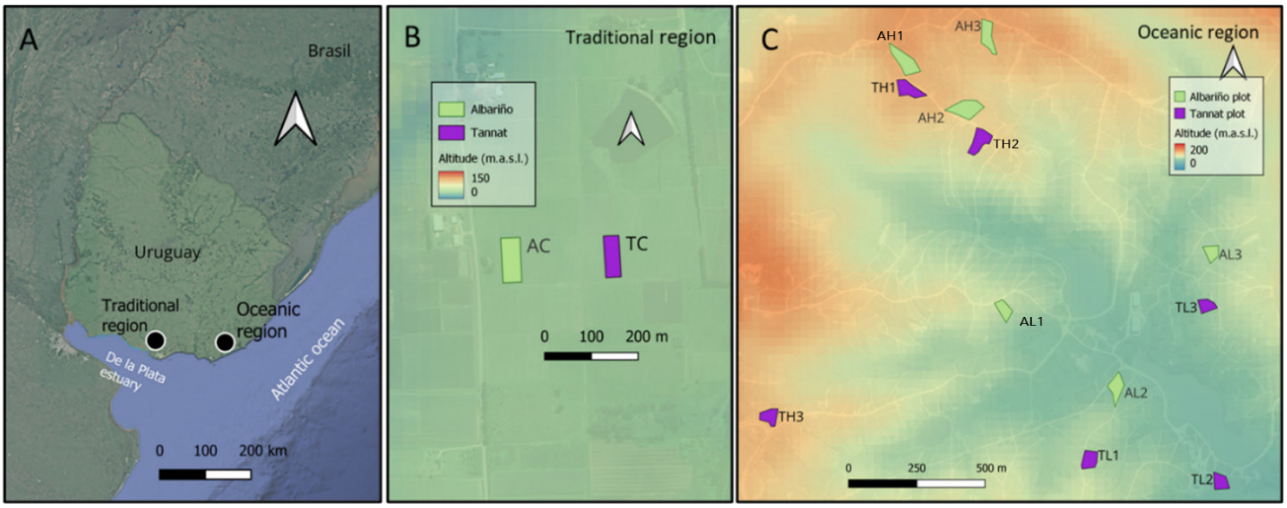


FIGURE 1. (A) Location of Uruguay within South America and location of the vineyards under study. (B) Location of reference plots in the traditional inland region. (C) Location of the 12 plots of Tannat and Albariño grouped according to altitude and exposure to the Atlantic Ocean: H = high altitude and exposed to the ocean, and L = low altitude and less exposed to the ocean.

exposure to oceanic influence: high-elevation plots (120–140 m.a.s.l.) with direct exposure to maritime conditions (designated as H), and low-elevation plots (70–95 m.a.s.l.) with more sheltered conditions (defined as L) (Figure 1C; Table 1). In the traditional inland region, plot C (one for each variety) was used as a reference for descriptive and comparative analysis with the oceanic plots (H and L). In particular, its values were contrasted exploratively with the average of the oceanic plots to contextualise the measurements and describe relative trends (Figure 1B; Table 1).

Vine performance was assessed in adult vineyard plots of *Vitis vinifera* L. cvs. Tannat and Albariño (Figure 1). In each plot, three subsamples of vine groups consisting of seven consecutive vines each were selected for agronomic, physiological, and metabolic assessments during the 2022–2023, 2023–2024, and 2024–2025 growing seasons (hereafter referred to as 2023, 2024, and 2025, based on the harvest year).

2.1 Assessment of vegetative development, yield components, and plant balance

To evaluate the vine performance, the following parameters were obtained by measuring seven plants per subsample: yield (kg/ha), number of clusters per vine (CN), average cluster weight (CW), pruning weight, Ravaz index (RI; Ravaz, 1911), potential exposed leaf area (SFEp; Carbonneau, 1983) and the SFEp/Yield ratio. The incidence of Botrytis cinerea-infected clusters (BCI) was estimated by visual assessment of symptom presence on grape clusters. For calculations, the total weight of clusters classified as infected was recorded. Bud fertility (BF) was assessed pre-flowering by counting the number of inflorescences per shoot and categorised according to bud position on the cane: basal (nodes 1–2), medium (nodes 3–4), and apical (nodes 5–6).

2.2 Evaluation of physiological parameters

Gas exchange assessments were carried out at specific, representative time points to characterise the state of the plants under the prevailing environmental conditions. Gas exchange parameters were measured in six reference plots representing site-specific conditions for both cultivars (TL2, TH2, TC, AH3, AL2, and AC). Measurements included net CO_2 assimilation rate (A), transpiration rate (E), stomatal conductance to water vapour (gsw), leaf vapour pressure deficit (VPDleaf), internal-to-ambient CO_2 ratio (Ci/Ca), and leaf temperature by contact (TleafCnd). For each plot, nine leaves were measured (three per subsample), including one leaf each from the basal, middle, and apical parts of the canopy. Measurements were conducted between veraison and harvest on clear days with maximum temperatures above 28 °C, around solar noon (12:00 local time). In 2023, measurements were conducted on January, 17 (C plots) and January, 26 (H and L plots); in 2024, on January, 24 and February, 28 (H and L plots), and January, 29 (C plots); and in 2025, on January, 29 and February, 24 (C plots), and February, 10 and March, 5 (H and L plots). An infrared gas analyzer (IRGA, LI-6800, LI-COR Biosciences, Lincoln, NE, USA) was used under controlled conditions (relative humidity 60 %, CO_2 concentration 400 $\mu molmol^{-1}$ and incident light 1000 $\mu molm^{-2}s^{-1}$), while leaf temperature was left unmodified. Water use efficiency (WUE) was calculated as the ratio between net CO_2 assimilation (A) and the transpiration rate (E).

2.3 Description of berry metabolic compounds

Grape primary metabolites were assessed weekly from veraison to harvest using 50 randomly selected berries per subsample, following the OIV protocols (OIV, 2009). We measured total soluble solids (TSS, g/L) by refractometry (Hanna® HI 96801)

TABLE 1. Soil, topographic, and row orientation characteristics of the 14 selected Tannat and Albariño plots.

Plot ID	Variety	Site	Altitude (m.a.s.l.)	Slope (%)	Aspect (°)	Row orientation	Soil type	Soil depth (cm)
TH1	Tannat	H	136	5.9	214	N–S	Argiudoll	91
TH2	Tannat	H	124	10	131	SE–NW	Argiudoll	82
TH3	Tannat	H	135	9.9	32	E–W	Argiudoll	90
TL1	Tannat	L	94	9	95	N–S	Argiudoll	72
TL2	Tannat	L	72	5.8	151	E–W	Argiudoll	77
TL3	Tannat	L	89	6.7	292	SE–NW	Argiudoll	93
TC	Tannat	C	41	1.5	310	N–S	Hapludert	102
AH1	Albariño	H	138	9.4	109	N–S	Argiudoll	88
AH2	Albariño	H	120	9.3	46	E–W	Argiudoll	70
AH3	Albariño	H	138	8.5	165	SE–NW	Argiudoll	91
AL1	Albariño	L	92	12	145	SW–NE	Argiudoll	81
AL2	Albariño	L	77	5.4	345	E–W	Argiudoll	75
AL3	Albariño	L	88	4.8	173	N–S	Argiudoll	92
AC	Albariño	C	44	1	35	N–S	Hapludert	98

and pH by potentiometry (Oakton® 11 series pH meter). Titratable acidity (TA, g sulfuric/L), α-amino compounds (mg/L), and organic acids (malic and tartaric acids, g/L) were measured by OENOFOSS® analysis. Berry weight (BW, g) was also recorded. Soluble solids per berry were calculated as: TSS (g/berry) = TSS (g/L)*berry weight (g)/(0.0046*°Brix+0.9927)/1000 and yield-based weighting to obtain per-hectare values, as follows: TSS (kg/ha) = TSS (g/L)*0.75 L must/kg grape*Yield (kg/ha)/1000. The same procedure was performed to obtain values of malic and tartaric per hectare.

Secondary metabolites were analysed using the Glories and Agustin (1992) extraction method, as modified by González-Neves *et al.* (2004), on samples of 250 berries randomly collected per subsample. For Tannat, extractable anthocyanins at pH 1 (A pH 1), extractable anthocyanins at pH 3.2 (A pH 3.2), and total polyphenol index (TPI) were measured. The percentage of extractability (%EA) was calculated as: ((A pH 1–A pH 3.2)/A pH 1)*100. For Albariño, only TPI was determined. Spectrophotometric readings were taken using a GENESYS™ 180 UV-Vis spectrophotometer (Thermo Scientific™, Waltham, MA, USA).

3. Climate data collection

To assess the relationship between vine performance and local temperature, a TinyTag Data Logger (Gemini, Chichester) temperature sensor was installed in each of the 14 vineyard plots. These sensors recorded hourly air temperature from September the 1st to April the 30th during the 2023, 2024, and 2025 growing seasons. The average hourly temperature evolution was analysed and plotted using calendar-based windows that approximate the main phenological periods. These dates do not represent exact phenological stages for each variety or site; rather, they reflect the average timing of these stages across the varieties in our study: budburst to flowering (1st September to 31st October), flowering to veraison (1st November to 14th January), and veraison to harvest (15th January to 15th March).

Each growing season was classified according to the Southern Oscillation phase, El Niño (NO), La Niña (NA), or Neutral (NE), based on data from the National Oceanic and Atmospheric Administration (National Weather Services – NOAA, 2025), where 2023 corresponded to a La Niña, 2024 to an El Niño, and 2025 to neutral conditions. Precipitation was obtained from two meteorological stations of reference for each region: the Rocha INUMET (Uruguayan National Institute of Meteorology) station (34°49’ S, 54°31’ W; 20 m.a.s.l., located 30 km from the oceanic vineyards), and the INIA Las Brujas agroclimatic station (34°40’ S, 56°20’ W; 24 m.a.s.l., located 12 km from the traditional vineyards).

4. Data processing and statistical analysis

Vine responses were analysed separately for Tannat and Albariño using a linear mixed-effects model in SAS® (PROC MIXED; SAS Institute Inc., 2025). Growing season (GS: 2023, 2024, and 2025), oceanic site (H = high ocean exposure; L = low ocean exposure), and their interaction (GS × Site) were included as fixed effects. The experimental unit was the vineyard plot within the site; measurements taken at three centres within each plot were treated as subsamples and averaged to obtain a single plot mean per growing season. Because the same plots were evaluated across the three seasons, repeated measurements over time were accounted for by modelling GS as a repeated factor within plot using a compound symmetry covariance structure. Plot nested within site was included as a random effect, and denominator degrees of freedom were estimated using the Kenward–Roger. Multiple comparisons among factor levels were performed using the Tukey method, based on least squares means (LSMEANS), with a significance level set at $\alpha = 0.05$. In addition, plot C was used only as a descriptive reference for exploratory comparison with the oceanic plots and was not included in the inferential mixed-model analysis.

Evolution graphics for berry metabolite evolution were constructed using site-level means (H, L, and C), separately for each growing season. Additionally, radar plot representations based on representative berry metabolites were generated using site, year, and variety data to compare the metabolic profiles of the berries visually. A multivariate principal component analysis (PCA) based on *z*-score standardised data was performed to evaluate the variability of the observations in relation to spatial factors (H, L, and C) and temporal factors (growing seasons) as expressed by the agronomic and berry metabolic response variables. Graphical analyses were performed using OriginPro software (OriginLab Corporation, Northampton, MA, USA).

RESULTS

1. Climatic characterisation of growing seasons and sites

During the La Niña (2023), total rainfall was 189 mm recorded in the traditional inland region and 380 mm in the oceanic region. Rainfall was unevenly distributed across phenological stages: from budburst to flowering, 47 mm fell in the traditional inland region and 205 mm in the oceanic; from flowering to veraison, 77 mm and 73 mm, respectively; and from veraison to harvest, 65 mm and 102 mm. El Niño (2024) exhibited a total of 568 mm in the traditional inland region and 658 mm in the oceanic region. Rainfall was distributed: 205/247 mm (budburst – flowering), 161/196 mm (flowering – veraison), and 202/215 mm (veraison – harvest) in the traditional and oceanic regions, respectively. Under ENSO neutral conditions (2025), total rainfall was 420 mm in the traditional inland region and 460 mm in the oceanic region. Rainfall by phenological stage was 113/104 mm from budburst to flowering, 140/164 mm from flowering to veraison, and 166/192 mm from veraison to harvest, respectively (Figure 2).

Temporally, the 2023 season was warmer than 2024 by an average of +2.1 °C per hour during this period. The hourly mean temperature profiles reveal a distinct diurnal maximal temperature pattern between regions. In the oceanic region, peak temperatures consistently occurred between 12:00 and

13:00 local hour (LH) across all three phenological stages analysed. In contrast, the traditional inland region showed peak temperatures later in the day, typically between 15:00 and 16:00 LH. During the ripening period (veraison to harvest), this temporal shift in peak temperature results in a higher average temperature of +2.5 °C per hour between 12:00 and 18:00 LH in the traditional inland region compared to the oceanic sites. The combination of site and season effects revealed differences of up to 4 °C per hour, with site C in 2023 showing the highest mean temperature difference of 4.7 °C at 17:00 LH compared to site H. Similar patterns were observed during the flowering – veraison phase, with site C presenting on average +1.5 °C per hour higher temperatures across all years compared to site H, and 2023 being warmer than 2024 by +2.4 °C per hour. During the budbreak – flowering period, site C also showed higher hourly mean temperatures (+1.0 °C/h) compared to site L and the 2025 season was warmer by +2.2 °C/h compared to both 2023 and 2024 (Figure 3).

2. Physiological response in Albariño and Tannat

The Albariño cultivar showed its highest net assimilation rate (A) in 2024, with a seasonal average of 10.7 $\mu molCO_2\ m^{-2}\ s^{-1}$. The comparison between sites, the representative plots of L exhibited the highest A values, followed by H and C (9.9, 7.8, and 4.2 $\mu molCO_2\ m^{-2}\ s^{-1}$ respectively). The most site-growing season combinations were plots in H and L in 2024, with means of 11.8 and 13.1 $\mu molCO_2\ m^{-2}\ s^{-1}$. The lowest net assimilation rates, ranging between 2.8 and 3.7 $\mu molCO_2\ m^{-2}\ s^{-1}$, were observed in 2025 at all sites and in 2023 at site C. The transpiration rate (E) followed the same spatial and temporal pattern as A, with the lowest average value recorded at site C (1.44 $mmolH_2O\ m^{-2}\ s^{-1}$)

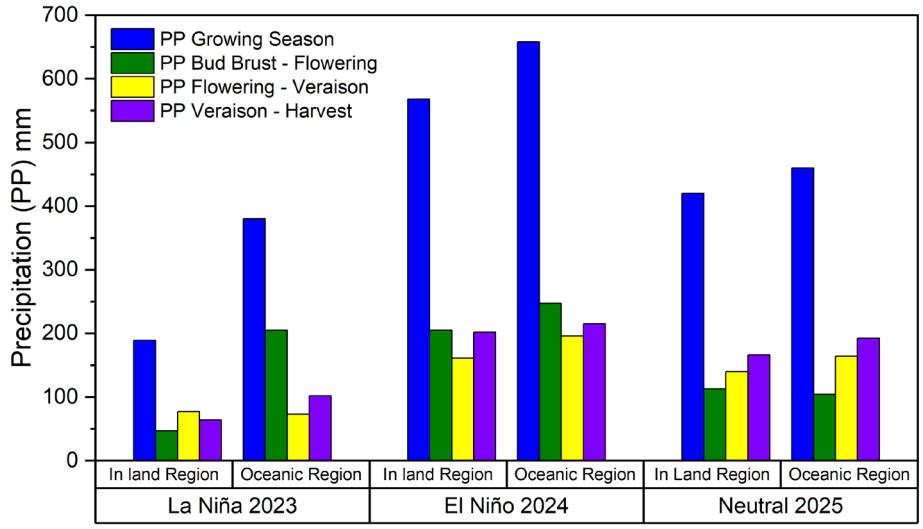


FIGURE 2. Precipitation during the growing seasons under La Niña (2023), El Niño (2024), and Neutral phase (2025) conditions for the traditional inland and oceanic wine-growing regions, divided by phenological stages: budburst to flowering, flowering to veraison, and veraison to harvest.

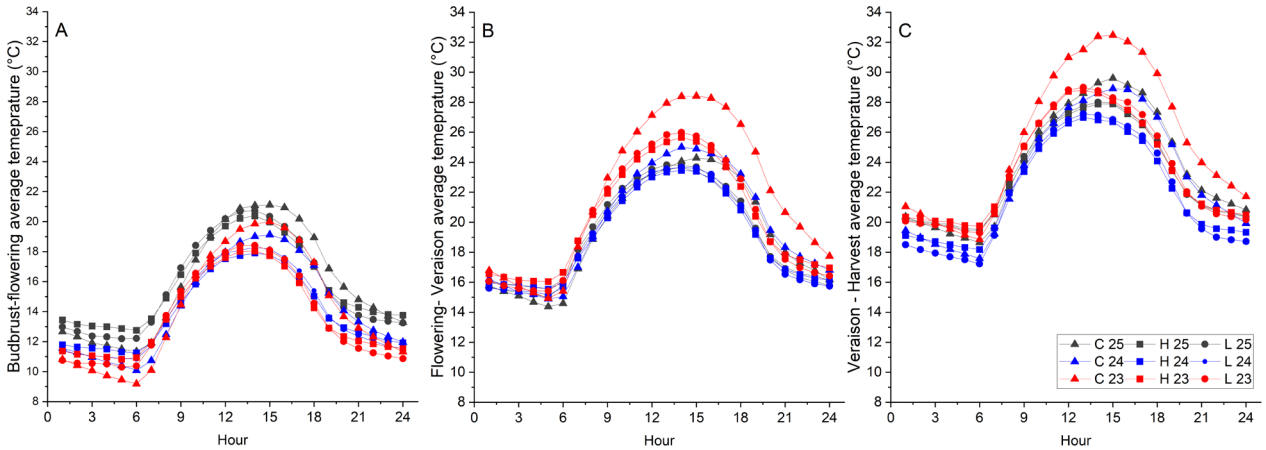


FIGURE 3. Hourly mean temperature (°C) evolution during three phenological phases: (A) budbreak to flowering, (B) flowering to veraison, and (C) veraison to harvest. Data are shown for high and exposed oceanic plots (H, squares), low and less exposed oceanic (L, circles), and traditional plots (C, triangles), across the 2023 (La Niña), 2024 (El Niño), and 2025 (Neutral) growing seasons.

and the minimum individual value of 0.87 mmolH_2O m^{-2} s^{-1} occurring at this site in 2025. Stomatal conductance (gsw) was higher in 2024 at sites H and L, reaching 0.188 and 0.217 mol m^{-2} s^{-1}, respectively, associated with a lower vapour pressure deficit at the leaf level (VPDleaf). The highest VPDleaf was observed at site C in 2023 (4.1 kPa), coinciding with stomatal closure, as indicated by low gsw values in 2023 and 2025 (0.047 and 0.035 mol m^{-2} s^{-1}, respectively).

Tannat variety reached its maximum net CO_2 assimilation rate in measures obtained in 2024, with an average of 11.4 µmolCO_2 m^{-2} s^{-1}. The H and L conditions showed the highest mean assimilation rates (7.9 and 9.0 µmolCO_2 m^{-2} s^{-1}, respectively), with maximum values in 2024 (13.3 and 13.5 µmolCO_2 m^{-2} s^{-1}, respectively). The lowest value was recorded at the plot in C in 2023 (2.6 µmolCO_2 m^{-2} s^{-1}). Transpiration rate (E) also peaked in 2024, with 3.70 mmolH_2O m^{-2} s^{-1}, while the lowest site-specific value was recorded at C in 2025 (0.7 mmolH_2O m^{-2} s^{-1}). Stomatal conductance remained relatively stable across growing seasons and sites, ranging from 0.030 to 0.087 mol m^{-2} s^{-1}, except for notable increases in plots L and H in 2024 (0.236 and 0.231 mol m^{-2} s^{-1}, respectively). The leaf-level vapour pressure deficit (VPDleaf) was lowest in 2024 (2.38 kPa) and highest in 2023 (3.30 kPa), with the most significant spatial values observed in site C (3.18 kPa), compared to L and H (2.61 and 2.79 kPa, respectively).

3. Agronomic and berry metabolic response of Albariño

The harvest duration across growing seasons and sites spanned 20 days, with the earliest date recorded in site C in 2023 (January the 30th) and the latest in sites H and L in 2024 (February the 19th). The average harvest dates in 2023, 2024, and 2025 were February the 6th, February the 17th, and February the 9th, respectively. By site, the mean harvest date was February the 5th in C, and February the 14th in H and L. The most remarkable intra-annual difference in harvest timing between sites occurred in 2023, with C being harvested 10 days earlier than H and L.

The agronomic performance of Albariño exhibited differences between growing seasons in terms of berry weight, with

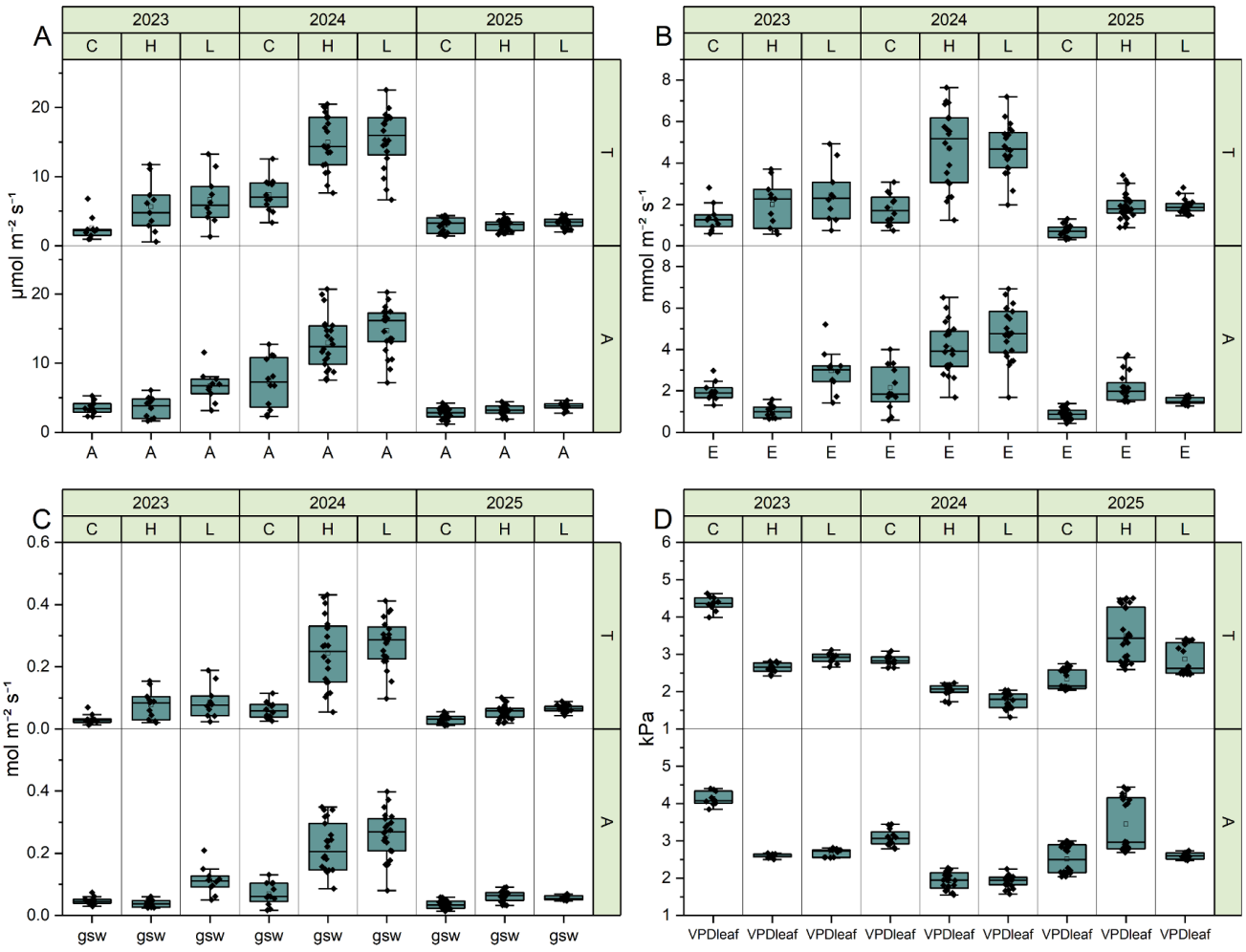


FIGURE 4. Physiological response assessed through measurements of: (A) net carbon assimilation rate (A), (B) transpiration rate (E), (C) stomatal conductance to water vapor (gsw), (D) leaf-level vapor pressure deficit (VPDleaf)), for Tannat (T) and Albariño (A) cultivars for high and exposed oceanic plots (H), low and less exposed oceanic plot (L), and traditional plot (C) across the 2023 (La Niña), 2024 (El Niño), and 2025 (Neutral) growing seasons.

a difference of 0.16 g higher in 2025 than in 2024. Between oceanic sites, differences were only associated with cluster weight (CW). The traditional inland reference plot (C) showed the largest differences compared to the two oceanic sites in Cw (62 g bigger in C), CN (8 cluster/plant lower in C), SFEp (33 % lower in C), RI (2.9 in oceanic plot *vs* 3.9) and basal bud fertility (42 % higher in C). In detail, bud fertility increased toward the apical position at all sites. Average bud fertility in the oceanic region ranged from 1.5 to 1.6 clusters per bud, compared to 1.9 in site C. This superiority was consistent across cane positions, with the basal nodes showing the greatest difference, up to 0.6 additional clusters per bud relative to H (Table 2).

Berry metabolite composition differed across growing seasons, where significant differences were found in α-amino, with 2025 showing +50 mg/L compared to 2023; titratable acidity which was +2.2 g/L higher in 2023 relative to 2025; TSS per berry (+0.037 g/berry in 2025 compared to 2024); and the total polyphenol index (TPI) with 2025 registering 21 units more than 2023 and 2024. In terms of the composition of organic acids, malic acid varied significantly depending on the growing seasons, while tartaric acid remained stable, thereby affecting the tartaric/malic ratio. When expressed as kg/ha, malic acid was most abundant in 2024, with an average of 16 kg/ha more than in 2023 and 2025. In the oceanic plot, malic acid was the only compound measured that showed differences, with H plots presenting 0.95 g/l more, significantly affecting the tartaric/malic ratio. Compared to the descriptive reference plot in the traditional region inland (C), differences were observed in malic acid (1.8 g/L lower in C), the tartaric/malic ratio (52 % higher in C) and the TSS/TA ratio (51 % higher in C) (Table 2).

The evolution of total soluble solids per berry (Figure 5A) showed maximum accumulation in 2025 at plot C, reaching 0.312 g/berry, while the lowest value was observed in 2024 at site L (0.244 g/berry). A linear accumulation trend was observed in 2024 and 2025, whereas in 2023, TSS accumulation slowed in the final days of ripening. The onset of TSS accumulation occurred later in 2024 than in the 2023 and 2025 growing seasons. When evaluating TSS as g/L (Figure 5B), the highest value was recorded in 2025 at C (237 g/L) and the lowest in 2024 at H (206 g/L). In both 2024 and 2025, sites H and L reached a plateau approximately one week before harvest, whereas site C did not exhibit this plateau. In 2024, H and L eventually achieved levels similar to 2023 and 2025, although a week later.

The degradation kinetics of malic acid showed a rapid decline in all three years at site C, whereas H and L displayed a slower degradation rate, especially toward the end of the ripening period. Across all seasons, malic acid degradation was consistently slower in H compared to L, with the difference being most pronounced in 2025, where H surpassed L by 1.6 g/L at harvest. The combination of acidity and sugar levels influenced the TSS/TA ratio (Figure 5C), with the highest ratio found in 2024 at C (60), more than twice the value observed at L in 2023 (28). The smallest difference between sites occurred in 2025 (12.5 units), while the greatest was in 2023 (27.4 units).

4. Agronomic and berry metabolic response of Tannat

The average harvest date in site C was February, 25, while in the oceanic plots (H and L) it occurred on March, 8, representing a difference of 11 days. Across vintages, the mean harvest dates were February, 24 for 2023, March, 14 for 2024, and March, 3 for 2025. In 2023, site C advanced harvest by 14 days compared to the oceanic plots. The combination of the earliest (February, 15, 2023, in site C) and the latest harvest date (March, 19, 2024, in sites H and L) resulted in a total harvest window of 32 days.

Among the evaluated growing seasons, 2025 presented the lowest cluster weight (–131 g) compared to the mean of the previous growing season. In 2023, the cluster number was reduced by 5 compared to the 2024 and 2025 average (17 clusters). Consequently, 2024 recorded the highest yield and the greatest incidence of *Botrytis cinerea* rot, with 9596 kg/ha and 2862 g/plant more than the average of the other seasons, respectively (Table 3). Differences between oceanic sites were found in cluster weight (Cw). The comparison with the traditional inland region (C) showed, on average, 0.25 g lower berry weight and 8.7 fewer clusters, resulting in a yield reduction of 9605 kg/ha compared to the average of the oceanic plots. Leaf area was also lower in region C, with 1997 m^2/ha less than oceanic plots, resulting in a 31 % difference in IR and a 22 % change in SFEp/Yield.

Regarding berry metabolites at harvest by growing season, α-amino compound concentration was lowest in 2024, followed by 2025 (+79 mg/L) and 2023 (+96 mg/L). In contrast, tartaric acid concentration was highest in 2024 (9.2 g/L), followed by 2025 (7.6 g/L) and 2023 (6.1 g/L). Malic acid concentration was lowest in 2024, followed by 2025 (+0.8 g/L) and 2023 (+1.1 g/L). However, when malic acid was adjusted by yield, no significant differences were found among growing seasons. The highest soluble solids concentrations were recorded in 2023 and 2025. Nevertheless, accumulation per berry was highest in 2025 (+0.039 g/berry), which was also reflected in the yield-adjusted accumulation, with 2358 kg/ha more than the 2023 and 2024 averages. Potentially extractable anthocyanins (A pH 1) presented the highest concentration in 2025 (+938 mg/L compared to 2023). Anthocyanin extractability in 2024 was 12 % lower than in the other growing seasons (Table 3).

Site-specific differences between the oceanic plots in berry metabolites at harvest were observed for malic acid, which was significantly higher in H (+0.95 g/L), resulting in a significant shift in the tartaric/malic ratio. Anthocyanins (A pH 1) were significantly higher in L (+732 mg/L), in association with a 9 % higher extractability index. The traditional inland region (C) exhibited trends in differences in α-Amino compounds (60 % higher in C), malic acid (24 % lower in C), and anthocyanins (17 % lower in C). When adjusted for yield, malic acid accumulation reached 52 kg/ha in H, 32 kg/ha in L, and 14 kg/ha in C.

Soluble solids concentration was 10 g/L higher in plot C compared to H. However, accumulation, expressed as grams of soluble solids per berry, was lower by 0.044 g/berry. This trend was consistent when results were yield-adjusted per hectare, with the average of H and L accumulating 2,097 kg/ha more soluble solids than region C.

The highest concentration of total soluble solids (TSS) was recorded in plot C in 2023, reaching 259 g/L, while the lowest was observed in plot C in 2024 (221 g/L) (Figure 6B). This contrasts with the accumulation of soluble solids per berry, where the highest value occurred in H in 2025 (0.395 g/berry) and the lowest in C in 2024 (0.277 g/berry). The kinetics of soluble solids accumulation revealed several periods during ripening in which weekly accumulation was negligible. This stagnation was particularly evident in 2023 and 2025. Following this detention, berry sugar accumulation resumed (Figure 6A).

TABLE 2. Agronomic parameters and berry metabolite composition at harvest for Albariño during 2023 (La Niña), 2024 (El Niño), and 2025 (Neutral) growing seasons in the oceanic plots, high exposure (H) and low exposure (L). The inland plot C is shown as a descriptive reference.

		Oceanic sites			Growing season				Interactions	Inland reference (descriptive)	Δ = Oceanic mean – C	
		H	L	*p*-value	2023	2024	2025	*p*-value	(Site x GS)	C	Value	% Difference relative to ocean mean
Agronomical responses	BW (g)	1.37	1.36	ns	1.34 b	1.29 b	1.45 a	0.004	ns	1.32	0.05	3
	CW (g)	111	90	0.04	105	109	89	ns	ns	162	–62	–61
	CN	20.0	20.2	ns	18.4	21.2	20.6	ns	ns	12	8.1	40
	Yield (kg/ha)	11,189	9,048	ns	9,473	11,844	9040	ns	ns	8,031	2,088	21
	BCI (g/pl)	0	0	ns	0	0	0	ns	ns	0	0	0
	SFEp (m^2/ha)	7,673	7,228	ns	7,103	7,886	7,362	ns	ns	4,974	2,477	33
	SFEp/Yield	0.75	0.86	ns	0.80	0.74	0.88	ns	ns	0.63	0.18	22
	RI	3.0	2.8	ns	3.1	3.3	2.3	ns	ns	3.9	–1	–34
	Basal BF	1.1	1.3	ns	1.3	1.2	1.1	ns	ns	1.7	–0.5	–42
	Middle BF	1.7	1.8	ns	1.8	1.7	1.7	ns	ns	1.9	–0.2	–9
	Apical BF	1.7	1.8	ns	1.8	1.7	1.8	ns	ns	2	–0.3	–14
Berry metabolic responses	TSS (g/L)	210	215	ns	214	211	213	ns	ns	229	–17	–8
	TSS (g / berry)	0.265	0.267	ns	0.263 ab	0.249 b	0.286 a	0.021	ns	0.275	–0.009	–3
	TSS (kg/ha)	2,192	1,800	ns	1,918	2,284	1,788	ns	ns	1602	394	20
	pH	3.09	3.09	ns	3.08	3.12	3.07	ns	ns	3.24	–0.15	–5
	TA (g sulfuric/L)	6.4	5.8	ns	7.4 a	5.7 b	5.2 b	0.0001	ns	4.2	1.9	31
	Tartaric acid (g/L)	8.3	8.2	ns	8	8.2	8.5	ns	ns	7.9	0.2	4
	Tartaric acid (kg/ha)	70	56	ns	57	73	58	ns	ns	48	15	24
	Malic Acid (g/L)	5.4	4.5	0.04	4.9 ab	5.5 a	4.5 b	0.028	ns	3.1	1.8	37
	Tartaric/ Malic	1.59	1.94	0.03	1.70 b	1.56 b	2.00 a	0.006	0.031	2.69	–0.93	–52
	Malic acid (kg/ha)	45	30	0.023	34 b	48 a	30 b	0.013	ns	18	20	52
	TSS/TA	34	39	ns	30 b	38 a	42 a	0.0009	ns	55	–19	–51
	α-Amino (mg/L)	131	118	ns	98 b	131 a	148 a	0.002	ns	149	–25	–20
	TPI	41	44	ns	35 b	35 b	56 a	0.002	ns	41	1	2

Abbreviations: BW: berry weight, CN: cluster number, CW: cluster weight, BCI: cluster affected by *Botrytis cinerea* at harvest, SFEp: potential exposed leaf area, RI: Ravaz index, BF: bud fertility, TA: titratable acidity, TSS: total soluble solids, TPI: total polyphenol index. Different letters indicate significant differences between growing seasons according to Tukey's test ($p < 0.05$). ns: not significant.

Titratable acidity reached its lowest value in C in 2023, being 2.4 g/L lower than the maximum observed in H in 2024. The degradation kinetics of acidity followed a similar pattern between oceanic plots, with a temporal shift of 7 to 10 days later compared to C. Moreover, C did not exceed TA concentration compared to H or L in any site–growing season combination (Figure 6D). Malic acid evolution followed a similar trend to titratable acidity; the highest concentration was recorded in H in 2023 and the lowest in C in 2024, with a difference of 2.5 g/L between them. In all growing seasons, malic acid concentrations in H consistently exceeded those in L, with H plots recurrently showing higher levels at harvest (Figure 6E). The TSS/TA ratio distinguished C from the oceanic plots (H and L) across the three growing seasons, with C in 2025 showing the highest value (90), while the 2023-site H combination exhibited the lowest value (39) (Figure 6C).

5. Spatial and temporal variability in the agronomic and metabolic response of Albariño and Tannat

Principal component analysis (PCA) revealed that in Tannat, PC1 accounted for 33.5 % and PC2 for 22.9 % of the variability, whereas in Albariño, PC1 accounted for 40.1 % and PC2 for 15.4 % (Figure 7). In Tannat, a grouping by growing seasons was observed in 2025 across all sites, mainly associated with TPI, TSSb, berry weight (BW), A pH 1, TSS/TA, TSS, and malic acid. However, in 2023 and 2024, the grouping was fragmented by site, particularly between oceanic parcels (H and L) and inland parcels (C). Inland parcels were positively discriminated by TSS, higher TSS/TA ratio, higher extractability (lower %EA), and α-amino acids, whereas oceanic parcels were associated with TSSb, A pH 1, malic acid, tartaric acid, titratable acidity (TA), yield, SFEp, RI, PRw, CN, and Y/SFEp (Figures 7A and 7B).

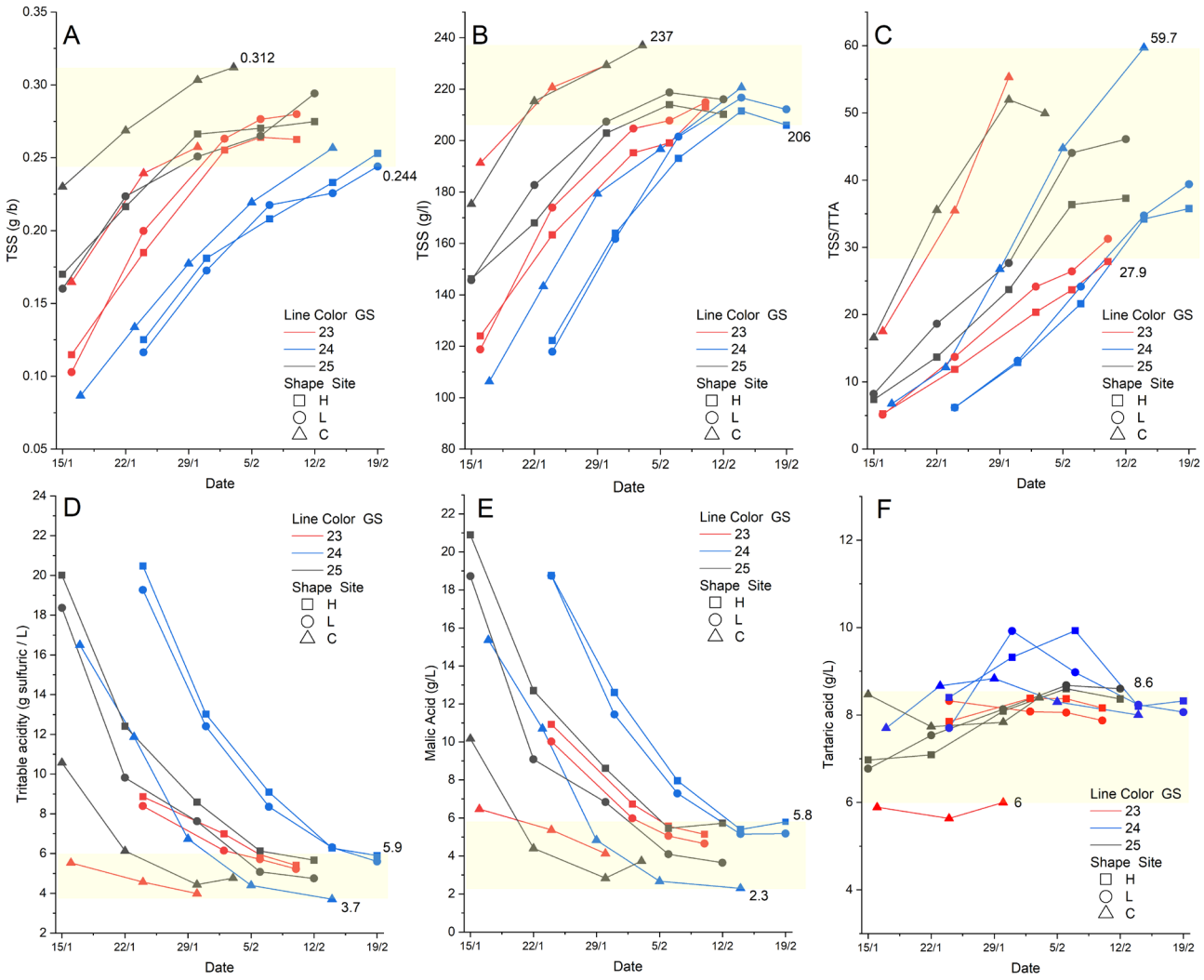


FIGURE 5. Evolution of Albariño berry metabolites during the ripening period: (A) total soluble solids per berry (TSS, g/b), (B) total soluble solids per litre (TSS, g/L), (C) TSS to titratable acidity ratio (TSS/TA), (D) titratable acidity (TA, g tartaric acid/L), (E) malic acid (g/L), and (F) tartaric acid (g/L) across the three sites: high and exposed oceanic plots (H), low and less exposed oceanic plot (L), and traditional inland region (C), for the 2023 (La Niña), 2024 (El Niño), and 2025 (Neutral) growing seasons.

The yellow background indicates extreme differences at harvest between growing season-site combinations.

TABLE 3. Agronomic parameters and berry metabolite composition at harvest for Tannat during 2023 (La Niña), 2024 (El Niño), and 2025 (Neutral) growing seasons in the oceanic plots, high exposed (H) and low exposed (L). The inland plot C is shown as a descriptive reference.

		Oceanic sites			Growing season				Interactions	Inland reference (descriptive)	Δ = Oceanic mean – C	
		H	L	*p*-value	2023	2024	2025	*p*-value	(Site x GS)	C	Value	% Difference relative to ocean mean
Agronomical responses	BW (g)	1.71	1.61	ns	1.60	1.63	1.74	ns	ns	1.41	0.25	15
	CW (g)	269	222	0.04	242 b	302 a	171 c	0.0006	ns	332	–86	–35
	CN	14.7	15.7	ns	11.7 a	17.4 b	16.5 ab	0.03	ns	6.5	9.0	57
	Yield (kg/ha)	1,9384	17,008	ns	13,254 b	23,285 a	14,124 b	0.0002	ns	8,591	9605	53
	BCI (g/pl)	1,363	597	ns	72 b	2,898 a	0 b	0.0056	ns	0	980	100
	SFEp m^2/ha	5,797	5,520	ns	5,193	6,070	5,714	ns	ns	3,661	1,997	35
	SFEp/Yield	0.33	0.39	ns	0.39 b	0.22 a	0.41 b	<.0001	ns	0.44	–0.08	–22
	RI	11.8	12.4	ns	8.5 a	13.9 b	11.2 ab	0.03	ns	8.4	4.0	31
	Basal BF	1.2	1.2	ns	1.3	1.3	1.1	ns	ns	1.3	–0.1	–8
	Middle BF	1.7	1.8	ns	1.8	1.7	1.7	ns	ns	1.6	0.2	11
	Apical BF	1.8	1.9	ns	1.9	1.7	1.8	ns	ns	1.8	0.1	5
Berry metabolic responses	TSS (g/L)	232	240	ns	236 ab	231 b	242 a	0.02	ns	243	–7	–3
	TSS (g/berry)	0.362	0.351	ns	0.343 b	0.344 b	0.383 a	0.0008	ns	0.318	0.039	11
	TSS (kg/ha)	4,186	3,767	ns	2,965 b	5,378 a	3,072 b	0.0001	ns	1,879	2,098	53
	pH	3.32	3.22	ns	3.26 b	3.19 b	3.37 a	0.0005	ns	3.34	–0.07	–2
	TA (g sulfuric/L)	5.4	5.1	ns	5.8 b	6.8 a	3.2 c	<.0001	ns	4.1	1.1	21
	Tartaric acid (g/L)	7.4	7.9	ns	6.1 c	9.21 a	7.64b	<.0001	ns	7.3	0.4	5
	Tartaric (kg/ha)	112	105	ns	60 b	186 a	80 b	<.0001	ns	47	62	57
	Malic Acid (g/L)	3.7	2.8	0.0005	3.5 a	2.4 b	3.2 a	<.0001	ns	2.3	0.7	24
	Malic (kg/ha)	52	35	0.01	46	50	33	ns	ns	14	30	68
	Tartaric/Malic	2.3	3.6	0.0016	1.7 a	3.8 c	2.4 b	<.0001	0.01	3.5	–0.6	–19
	TSS/TA	54	59	ns	42 c	50 b	78 a	<.0001	ns	75	–19	–33
	α-Amino (mg/L)	97	82	0.02	127 a	31 c	110 b	<.0001	ns	143	–54	–60
	TPI	68	71.8	ns	63 b	55 c	92 a	<.0001	ns	66	4	6
	A pH 1 (mg/L)	2,611	3,343	0.013	2,505 b	2,977 ab	3,449 a	0.006	ns	2,467	510	17
	%EA (%)	53	62	0.012	60	63	50	0.0052	ns	57	1	2

Abbreviations: BW: berry weight, CN: cluster number, CW: cluster weight, BCI: clusters affected by *Botrytis cinerea* at harvest, SFEp: potential exposed leaf area, RI: Ravaz index, BF: bud fertility, TA: titratable acidity, TSS: total soluble solids, A pH 1: extractable anthocyanins at pH 1, %EA: extractability percentage, TPI: total polyphenol index. Different letters indicate significant differences between growing seasons according to Tukey's test ($p < 0.05$). ns: not significant.

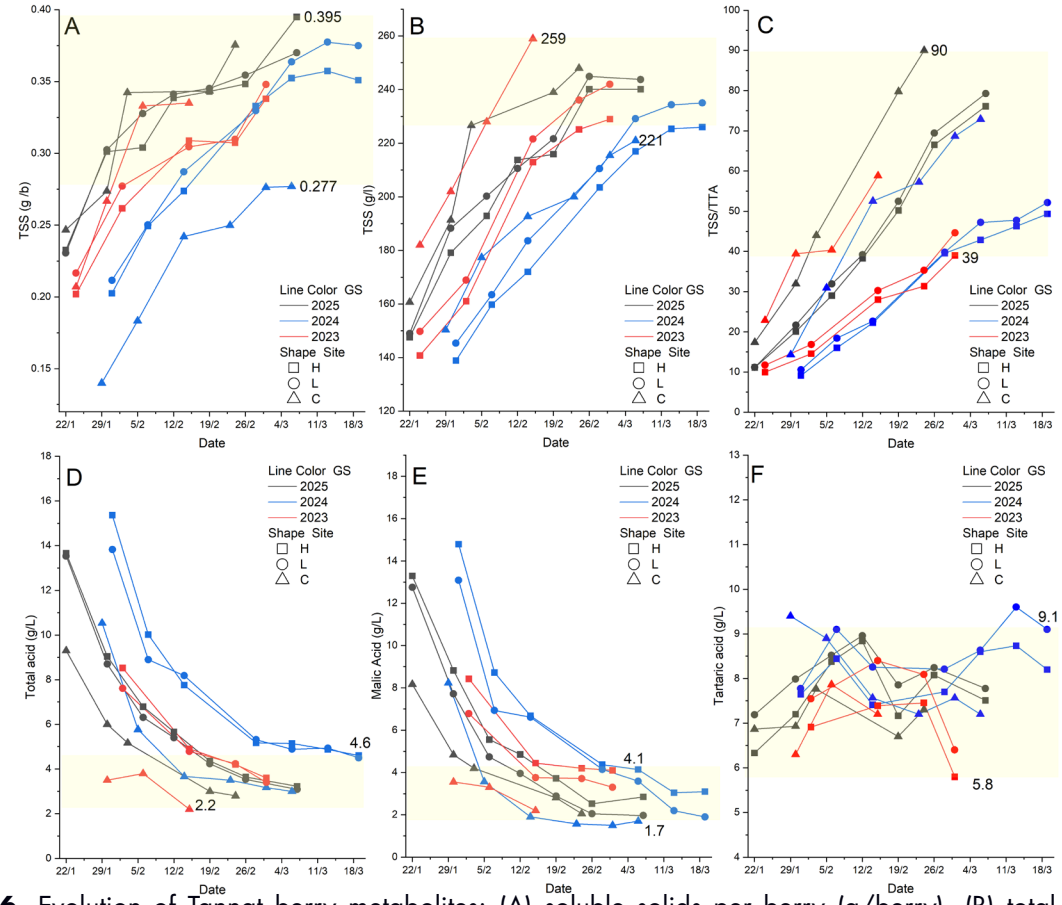


FIGURE 6. Evolution of Tannat berry metabolites: (A) soluble solids per berry (g/berry), (B) total soluble solids (TSS, g/L), (C) TSS to titratable acidity ratio (TSS/TA), (D) titratable acidity (g sulfuric /L), (E) malic acid (g/L), and (F) tartaric acid (g/L) across the three sites: high and exposed oceanic plots (H), low and less exposed oceanic plots (L), and traditional inland region (C), for the 2023 (La Niña), 2024 (El Niño), and 2025 (Neutral) growing seasons.

The yellow background indicates extreme differences at harvest between growing season-site combinations.

In Albariño, the separation of parcels followed a similar pattern to Tannat, but the spatial component (site: H, L, and C) was the strongest factor driving grouping. Inland parcels (C) were clearly separated to the right of PC1, while oceanic parcels (H and L) clustered to the left. Inland sites were mainly associated with TSS/TA, tartaric/malic ratio, TSS, cluster weight (Cw), pH, and RI, while oceanic sites were associated with tartaric acid, BW, shoot weight (ShootW), Y/SFEp, malic acid, PRw, and SFEp. Temporally, the 2025 season was separated along PC2 from the other growing seasons, driven by TPI, α-amino acids, TSSb, BW, and tartaric acid (Figures 7C and 7D).

DISCUSSION

1. Influence of climate on the physiology of Albariño and Tannat

Although this study aims to evaluate climatic influences and the oceanic imprint, the observed differences should be interpreted within the framework of integrated terroir systems (climate, soil, and management) and their interactions, avoiding attribution to climate alone. Nevertheless, the detailed analysis of the oceanic plots, which share comparable soil conditions and management practices, allows their contrasts to be interpreted more robustly. Furthermore, monitoring the same plots across climatically contrasting years (different ENSO phases) provides valuable information on cultivar behaviour in response to seasonal effects.

Climatic variability among growing seasons showed that 2023 experienced a 65 % reduction in precipitation compared to the historical average during the veraison period. In contrast, 2024 conditions were close to average, while 2025 was 23 % drier than usual (INUMET, 2025b). The 2023 season also recorded the highest maximum temperatures from flowering to harvest, whereas 2024 was the coolest. These climatic patterns align with previous findings, which describe La Niña seasons as typically dry and warm, and El Niño as temperate and humid (Cai *et al.*, 2020). The summer of 2023 presented particularly adverse thermal and water stress conditions for grapevines (Fourment & Piccardo, 2023), as corroborated by national reports (INUMET, 2023), which described the summer as a record in the last 42 years in terms of maximum temperatures and water deficit. However, these data should be interpreted as a characterisation of the climatic context, as no direct measurements of soil water status were available in the vineyards.

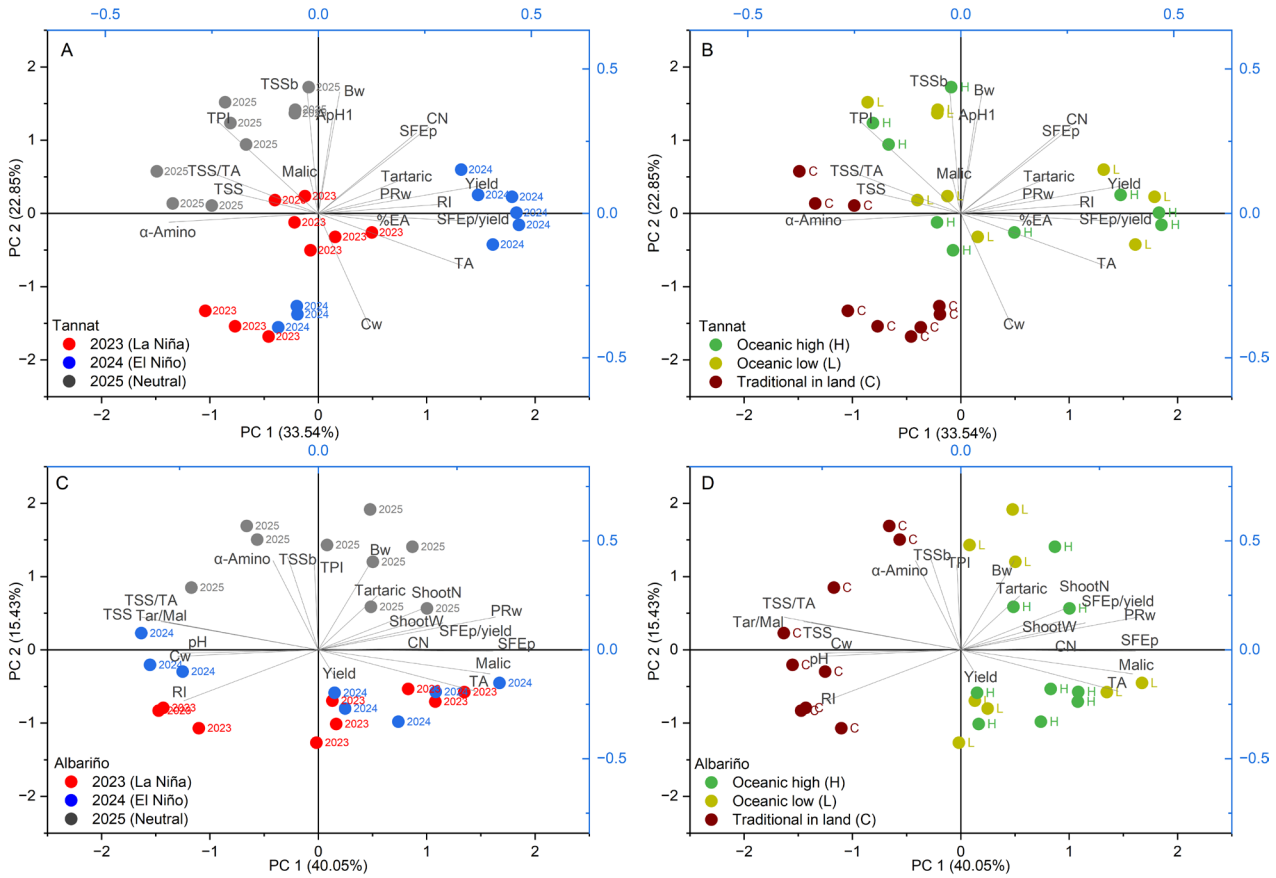


FIGURE 7. Principal component analysis (PCA) based on standardised agronomic and berry metabolic variables for Tannat (top) and Albariño (bottom). The left panels display the distribution of observations according to growing seasons (2023: La Niña, 2024: El Niño, 2025: Neutral), while the right panels show the distribution according to vineyard location (H: oceanic high, L: oceanic low, C: traditional inland).

Total soluble solids (TSS), the ratio of soluble solids to titratable acidity (TSS/TA), titratable acidity (TA), pH, tartaric and malic acids, α-amino nitrogen compounds, total polyphenol index (TPI), berry weight (BW), yield (Yield), number and weight of cluster (CN, CW), Ravaz index (RI), number and weight of shoots (ShootN, ShootW), potential exposed leaf area (SFEp), pruning weight (PRw) and ratio yield/SFEp (Y/SFEp).

The traditional inland region (C) was consistently warmer than the oceanic regions (H and L) throughout all phenological stages and vintages. Notably, temperatures in the oceanic region during the record-breaking summer of extreme heat were comparable to those observed in the traditional inland region during the El Niño temperature growing seasons. In 2023, the higher temperatures impacted site C more severely than the oceanic sites, as evidenced by the difference compared to 2024 and 2025. These findings highlight the ocean's buffering effect against extreme temperatures during ripening as reported and quantified by other authors (Bonnardot *et al*., 2002; Tachini *et al*., 2023, Tachini *et al*., 2026), supporting its potential role in climate change adaptation for viticulture.

Although the regions are separated by only 150 km, they are subject to different maritime influences. In the oceanic region, daily maximum temperatures occur around solar noon (12–13 LH), whereas in the traditional inland region, they are reached later in the afternoon (15–16 LH) as reported by Fourment *et al*. (2014). As a result, vines in the traditional inland region are exposed to both higher temperatures and longer durations of heat stress, which can alter physiological responses such as stomatal closure and reduce net photosynthesis. Identifying peak temperature hours also has practical implications for irrigation scheduling and agronomic management.

Climatic conditions also varied within growing seasons. 2023 did not start warm; during budburst, 2025 was actually the warmest period. However, from flowering onwards, 2023 developed into the hottest season. This highlights the importance of disaggregating phenological stages to better understand which phases of plant development are most affected by climate (Jones *et al*., 2012).

The plant's carbohydrate assimilation capacity is dynamic and responsive to water status and temperature (Greer & Weston, 2010). Despite a limited number of photosynthesis measurements (two dates per site per season), trends and values provided insight into the physiological status of both varieties during the ripening period, which serve as a descriptive reference. In measures obtained in 2024, the highest net CO_2 assimilation rates (A) were observed, coinciding with low atmospheric demand and high stomatal conductance. This favourable performance was especially

notable in the oceanic reference plots (H and L), where the absence of temperatures exceeding 35 °C and the possibility of presenting water available in the soil could allow higher net assimilation rates. In contrast, the 2023 and 2025 measures, particularly at site C, recorded the highest leaf vapour pressure deficits (VPDleaf), consistent with the thermal description. In relation to the plant, during the period of soluble solids accumulation, once the high-atmospheric-demand events recorded in 2023 and 2025 had passed, accumulation continued after a plateau. This pattern is consistent with a mainly transient limitation (*e.g.*, associated with stomatal closure under high VPD) rather than a chronic deterioration of the photochemical apparatus that persistently restricts carbon assimilation. However, since chlorophyll fluorescence was not measured, the contribution of non-stomatal limitations, such as possible chronic photoinhibition, cannot be completely ruled out (Chaves *et al*., 2010). The absence of differences in these parameters between 2023 and 2025 in relation to thermal description may be attributed to the fact that one of the measurements in 2025 was conducted during a heat wave, with temperatures exceeding the 90th percentile nationwide (INUMET, 2025a), which potentially affected the results. In this way, the particular conditions of the day can aggravate or mitigate the physiological state of the plant. As for the comparison between cultivars, they showed the same trend in response to climatic conditions. Future studies should incorporate more frequent and detailed assessments to better capture the dynamics and responses of varieties to stress events.

The 35 °C leaf temperature threshold was reaffirmed as a critical point beyond which photosynthesis is impaired (Greer & Weston, 2010; Torregrosa *et al*., 2017), directly linked to stomatal closure. This finding contributes novel data for Tannat and Albariño under Uruguayan conditions, where such records are scarce. It is also important to note that sun-exposed leaves can be up to 6.4 °C warmer than the ambient temperature (Kiaeian Moosavi *et al*., 2018), indicating that the canopy may experience more intense stress than inferred from air temperature alone. Nevertheless, below 35 °C, the significant variability in observed assimilation values suggests that other factors, such as water status, wind intensity, and nitrogen availability, may play a more substantial role in regulating photosynthesis (Hailemichael *et al*., 2016).

2. Climate conditions between growing seasons and sites impact agronomic behaviour and berry metabolic dynamics on Albariño

In our dataset, the inland reference (C) tended to show earlier harvest dates, where the combination of a warm site (traditional inland region) and a hot growing season (2023, La Niña) resulted in the earliest harvest recorded. Several studies have reported cycle shortening due to heat events linked to climate change, leading to rapid ripening and acid degradation, as shown in Figure 5, which can hinder aroma development, one of the primary quality parameters for white varieties (Fraga, 2020; van Leeuwen *et al*., 2024). However, extending the cycle in temperate growing seasons (as observed in 2024, mainly in C) was detrimental to acidity, as malic acid continued its decline, which is further accelerated under moderately warm conditions (25 °C) (Brandt *et al*., 2019).

Albariño yield remained stable across the three vintages, associated with a variation in berry weight of 0.16 g, despite expecting higher yields and berry weight in rainy growing seasons. At the oceanic sites, low bud fertility, particularly in basal buds, combined with reduced cluster weight, necessitated that the plants produce a greater number of clusters to achieve the desired yield. In contrast, this adjustment was not necessary in the traditional inland region, where higher bud fertility and larger cluster size, linked to greater water retention capacity of soils, prompted the agronomic decision to thin clusters to meet the target yield. The need for a greater number of clusters, linked to low bud fertility in the oceanic region, resulted in an increase in shoot number, which, combined with higher planting density, results in greater leaf area, despite being the soil with the lowest water retention capacity. The low bud fertility may be the result of lower incidental radiation at the time of induction due to a larger leaf area and/or lower total radiation in the oceanic region (Sánchez & Dokoozlian, 2005), and turning into a negative cycle. The increase in clusters has practical implications, including extended harvest durations and increased canopy management requirements. However, since Albariño is a white variety, a higher exposed leaf area (SFEp) may help mitigate excessive acid loss by maintaining bunch shading (Horák *et al*., 2021), as observed at oceanic sites. Furthermore, the vintage variation in precipitation and temperature did not result in significant changes in leaf area, bud fertility, or yield, indicating a high level of stability under contrasting climatic conditions. This is reflected in the plant balance indicator (SFEp/Yield), which ranged from 0.74 to 0.88, with no significant differences across the evaluated seasons. Thus, metabolic results in berries could not be directly linked to imbalances in vines between growing seasons.

High acidity and low alcohol are among the preferred traits in current wine markets, which become challenging under climate change conditions (Gutiérrez Gamboa & Fourment, 2024; Gutiérrez-Gamboa *et al*., 2021). In this study, titratable acidity, driven primarily by malic acid, was highest in the high and exposed oceanic plots (H) compared to L, due to slower degradation. This aligns with the characterisation of these sites as the coolest, linked to canopy development, maintaining temperatures that allow for malic acid preservation, changing the tartaric/malic ratio. The traditional inland region shows a tendency toward lower titratable acidity and malic acid concentration compared to oceanic sites, reflecting a possible association between high afternoon temperatures and, thus, accelerated malic acid degradation. Tartaric acid, which is less sensitive to temperature (Cholet *et al*., 2016), remained stable between 7.8 and 8.4 g/L across all sites and growing seasons, leading to a higher tartaric/malic ratio in the traditional inland region. In this way, the profile of organic acids may serve as an indicator to differentiate coastal terroirs in Uruguay linked to Albariño.

The evolution of TSS (g/berry) showed no plateau across ripening in any condition, indicating that extreme heat events did not reach levels capable of fully inhibiting

photosynthesis, as reported under extreme temperature stress (Greer & Weston, 2010; Pillet *et al*., 2015). The limited differences in soluble solids may reflect a relatively short ripening period, which reduces the plant's exposure to extreme heat and drought events during summer. The balance between sugars and acidity suggests that the oceanic region offers greater potential to produce balanced, high-acid wines with slower dynamic ripening. In the global context of climate change, where wines tend to exhibit higher alcohol and lower aroma and acidity, the oceanic region emerges as a promising area for Albariño cultivation, as suggested by Fourment *et al*. (2024).

3. Agronomic and berry metabolic response of Tannat to spatial and temporal variability

Among growing seasons, 2024 (El Niño) stood out as the most productive cycle, with yields nearly doubling due to significantly larger clusters (on average, 96 g heavier), consistent with rainfall and the possible availability of water in the soil. However, this increase in size, coupled with a humid and rainy climate, resulted in a 10 % incidence of *Botrytis cinerea* rot in the total production. The incidence of this fungus remains one of the main challenges for grape production in Uruguay during wet growing seasons, especially during the ripening period (Arrillaga *et al*., 2021). Unlike Albariño, which showed no signs of *Botrytis cinerea* infection across any of the growing seasons, Tannat, possibly due to its more extended ripening period and particular cluster morphology, did experience disease-related yield losses (Arrillaga *et al*., 2021; Ferrer *et al*., 2020). Despite the extreme conditions of 2023, neither the leaf area in the same growing season nor bud fertility in the following growing season was significantly affected, even though both parameters are tightly linked to temperature and water availability, showing the Tannat adaptation to climate variability (Sánchez & Dokoozlian, 2005).

α-amino compounds represent approximately 60 to 80 % of the total yeast assimilable nitrogen (YAN) required for proper fermentation of grapes (Verdenal *et al*., 2021). Therefore, α-aminonitrogen levels provide an indication of nitrogen availability for yeasts, but they are not definitive. Several authors suggest a threshold of 180 mg/L of YAN to ensure complete fermentation, while levels below 140 mg/L may be insufficient; therefore, the values observed in 2024 in the oceanic region may be problematic. In the rainy growing season, the marked increase in yield probably reduced α-amino compounds due to a dilution effect and higher N demand per unit of fruit, potentially amplified by N losses through leaching in sandy soil (Verdenal *et al*., 2021).

Despite the thermal differences between sites, the concentration of soluble solids varied by 0.6°*v/v* of probable alcohol between oceanic and traditional inland regions. The higher yields observed in the oceanic region did not penalise soluble solids at the berry. When expressed on a per-hectare basis (*i.e.*, yield-weighted), the oceanic vineyards showed greater TSS, indicating that the larger crop load was supported without a dilution of ripening. This pattern is consistent with a higher carbon supply capacity, in line with the temperature regime and the observed photosynthetic responses. Soluble solids concentrations (g/L) did not differ significantly between 2024 and 2025, although 2023 was notably dry (65 % below average). This likely led to sugar concentration via water loss, offsetting the effect of reduced yield. In contrast, 2025 showed higher sugar accumulation per berry and per hectare, indicating that moderate temperatures and possibly better soil water availability were conducive to sugar production, maintaining potential alcohol levels without yield loss. The evolution curves of sugar accumulation (g/berry) showed plateau phases during ripening, especially in 2023 and 2025, associated with elevated atmospheric demand and heat waves recorded in the region (INUMET, 2023, INUMET, 2025a). However, the vines resumed sugar accumulation once conditions improved, suggesting that no irreversible damage occurred, as reported in the literature under certain circumstances during extreme heat events. To confirm this, fluorescence analyses must be performed in the future. (Greer & Weston, 2010). Potentially extractable anthocyanins (A pH 1) revealed a greater potential for accumulation and maintenance of these compounds in the oceanic region, where significant differences were found in plots L. Anthocyanin is limited by temperatures above 30 °C and its accumulation is favoured by cool nights (Mori *et al*., 2005, Mori *et al*., 2007), highlighting the plant's climatic sensitivity expressed in berry composition. This finding is further supported when analysing anthocyanin yield per hectare (kg/ha), where vines maintained phenolic quality even under higher yield conditions.

Although titratable acidity did not differ among oceanic sites, the composition of organic acids varied, particularly in the tartaric/malic ratio. Malic acid was significantly higher in the high exposure oceanic site (H), consistent with observations in Albariño, reinforcing the ocean's moderating influence on temperature extremes and its role as a terroir-defining factor. The lower malic acid concentration observed in 2024, in a humid and temperate growing season in which the opposite would be expected, can be attributed to a delayed harvest in the oceanic plots. In fact, the 2024 growing season was harvested 10 days later than the average harvest date, which allowed continued malic acid degradation to occur, just like with Albariño. Detailed knowledge of acid composition is therefore crucial for decision-making regarding site-specific oenological objectives. Thus, cool oceanic conditions enabled the production of high-quality berries without a yield penalty. Consequently, a linear inverse relationship between yield and quality is not applicable when comparing regions; rather, the intrinsic terroir conditions must be considered to define the potential of each variety. Ferrer *et al*. (1997) proposed a Ravaz index range of 6 to 8 for Tannat in Uruguay; however, future studies should aim to refine site- and growing seasons-specific equilibrium indices to maintain vine stability under increasing climate variability and change.

4. What to expect from Albariño and Tannat under extreme heat growing seasons

The ability to link growing seasons with ENSO phases provides an early-season indication of how the viticultural cycle may develop, offering a degree of predictive certainty. These results during contrasting ENSO growing seasons can support the optimisation of key resources (such as irrigation management) and decision-making for the implementation of targeted vineyard management practices aimed at mitigating short-term adverse effects. However, to strengthen the reliability of these associations, further studies encompassing a greater number of growing seasons influenced by ENSO events are necessary to validate and refine these preliminary findings. Albariño and Tannat were mainly affected in terms of composition and organic acid content, as well as in their relationship with soluble solids; in Tannat, significant changes were also observed in anthocyanin levels. The remaining parameters did not differ significantly, nor was the 2023 average statistically different from those of 2024 or 2025. This also leads us to believe that there may be other parameters that are more sensitive than those measured in this study, such as secondary compounds, like aromas. Thus, the average increase of 2.1 °C in the maturity period during peak demand hours (12:00–18:00 LH) in what was a record-breaking summer for extreme temperatures in the country did not substantially alter the vine's physiological response. However, the combination of a warm site and a warm growing season (traditional inland region – 2023), particularly in Tannat, represented a possible impact scenario, reinforcing the oceanic zone's greater capacity for climate change adaptation. This further supports the need for a regionalisation strategy aligned with production goals and future climate scenarios.

Tannat is a cultivar that responds strongly to both spatial and temporal climatic variability (Ferrer *et al*., 2020; Fourment *et al*., 2017; Tachini *et al*., 2022). Therefore, it is imperative to continue investigating Tannat in order to develop harvest strategies that provide more stable products across vintages. This will enable producers to plan vineyard operations in advance, according to forecasted climatic conditions, in order to maximise site and vintage potential. In contrast, Albariño (characterised by a short ripening cycle and greater plasticity; Fourment *et al*., 2024) demonstrates more consistent performance across sites and seasons, making it a promising option for national growers seeking stability in both yield and quality. Lastly, it is essential to highlight that the irrigation system likely mitigated some of the impacts observed in 2023. This underscores the importance of emphasising the soil capacity and irrigation management as a key agronomic strategy in future studies (Pereyra & Ferrer, 2024), and also take into account a white cultivar as a new emblematic and adapted variety for Uruguayan conditions.

This study provides valuable insights for optimising harvest date decisions, as both excessively rapid and overly delayed ripening may lead to imbalances in key compositional parameters when waiting for other compounds to reach the desired levels, depending on site and variety. By studying the spatial and temporal sources of variability in berry agronomic and metabolic traits, the results highlight how terroir conditions and climatic variability influence the synchronisation of sugar accumulation, acidity degradation, and phenolic development. Such knowledge is essential to avoid trade-offs between technological and phenolic maturity, enabling site- and cultivar-specific harvest strategies that preserve grape quality.

Finally, the results demonstrate that the berry composition in Albariño and Tannat is influenced by both spatial variability (terroir) and temporal variability associated with interannual climatic conditions (ENSO). Albariño behaves more stably between production growing seasons, retaining its freshness and acidity. In contrast, Tannat was more strongly affected by interannual climatic variability, with distinct differences among dry (La Niña) years, wet (El Niño) years, and neutral years. These findings highlight the importance of considering both site selection and climatic variability in viticultural planning and in the adaptation of cultivars to climate change (Figure 8).

CONCLUSIONS

Over three climatically contrasting growing seasons linked to ENSO phases, this study shows that the growing season and local ocean conditions (H vs. L) can influence vine yield components and changes in berry metabolic profiles, thus addressing the objective of quantifying seasonal and site-related effects in ocean-influenced environments.

Cultivar responses differed; Albariño exhibited comparatively stable performance across growing seasons, while oceanic conditions, especially in the more exposed plots, favoured the preservation of malic acid, with consequences for the sugar/acid balance, supporting Albariño's suitability for maintaining freshness under variable seasons. In contrast, Tannat was more sensitive to interannual climatic variability, with quality risks emerging under the warmest combinations of site and season, whereas oceanic plots tended to buffer thermal pressure, supporting the objective of evaluating site-related buffering capacity under warming-relevant conditions. Within oceanic sites, metabolite contrasts suggest complementary responses (*e.g.*, higher malic acid in H and higher anthocyanins in L), highlighting the need for site-specific strategies to optimise technological *vs* phenolic maturity.

Finally, because regional contrasts integrate terroir systems (climate, soil, and management), these findings should be interpreted as evidence of integrated site and season responses rather than purely climatic product. Additional growing seasons associated with ENSO phases, as well as direct plant/soil water status measurements would further strengthen attribution.

ACKNOWLEDGEMENTS

We are grateful to the Comisión Académica de Posgrado (CAP) of the Universidad de la República for providing the PhD scholarship of Ramiro Tachini, and to the ClimatSUD Program, the ECOS-SUD program, the National Agency for Research

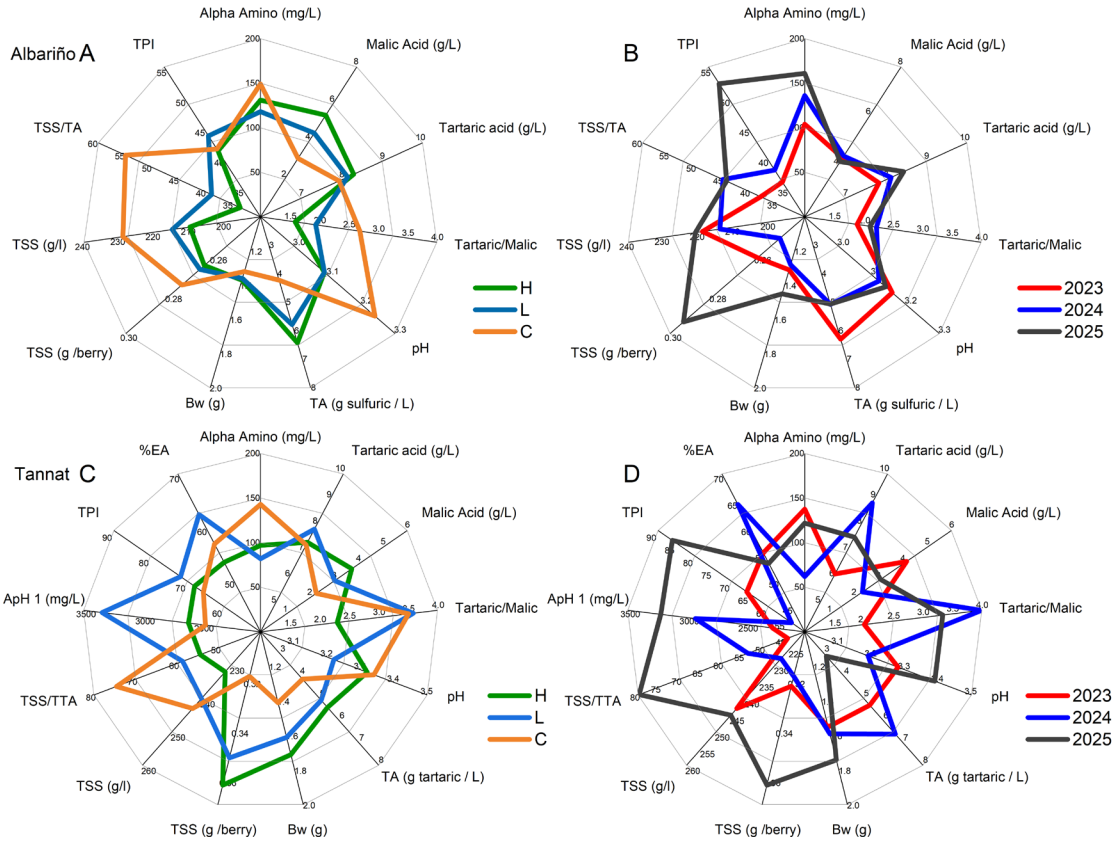


FIGURE 8. Berry composition profiles of Albariño based on (A) site of production (H: high and exposed oceanic plots, L: low and less exposed oceanic plots, and C: traditional inland region) and (B) growing seasons 2023 (La Niña), 2024 (El Niño), and 2025 (Neutral). Grape profiles of Tannat based on (C) site of production and (D) production growing seasons.

BW: berry weight, TA: titratable acidity, TTS: total soluble solids, A pH 1: anthocyanins extracted at pH 1, %EA: percentage extractability of anthocyanins, TPI: total polyphenol index.

and Innovation (ANII) and Bodega Garzón for their financial support. We also acknowledge Bodega Bouza (Eduardo Boido and Néstor Merino) and Bodega Garzón (Germán Bruzzone and Manuel Macchiavello) for their collaboration. We also thank the Instituto de Investigaciones Agropecuarias (INIA) and the Instituto Nacional de Meteorología (INUMET) of Uruguay for providing climatic data. Special thanks to Lucila Bentancor, Paula Rodríguez, Analía Hernández, Agustina Clara, and Nora López for their valuable support.

REFERENCES

Alem, H., Rigou, P., Schneider, R., Ojeda, H., & Torregrosa, L. (2019). Impact of agronomic practices on grape aroma composition: A review: Impact of agronomic practices on grape aroma composition. Journal of the Science of Food and Agriculture, 99(3), 975–985. https://doi.org/10.1002/jsfa.9327

Arrillaga, L., Echeverría, G., Izquierdo, B., Rey, J. J., Pallante, A., & Ferrer, M. (2021). Response of Tannat (Vitis vinifera L.) to pre-flowering leaf removal in a humid climate. OENO One, 55(2), 251–266. https://doi.org/10.20870/oeno-one.2021.55.2.4613

Bonnardot, V., Planchon, O., Carey, V. A., & Cautenet, S. (2002). Diurnal wind, relative humidity and temperature variation in the Stellenbosch-Groot Drakenstein winegrowing area. South African Journal of Enology & Viticulture, 23(2), 62–70.

Brandt, M., Scheidweiler, M., Rauhut, D., Patz, C.-D., Will, F., Zorn, H., & Stoll, M. (2019). The influence of temperature and solar radiation on phenols in berry skin and maturity parameters of Vitis vinifera L. cv. Riesling. OENO One, 53(2). https://doi.org/10.20870/oeno-one.2019.53.2.2424

Cai, W., McPhaden, M. J., Grimm, A. M., Rodrigues, R. R., Taschetto, A. S., Garreaud, R. D., Dewitte, B., Poveda, G., Ham, Y.-G., Santoso, A., & others. (2020). Climate impacts of the El Niño–southern oscillation on South America. Nature Reviews Earth & Environment, 1(4), 215–231. https://doi.org/10.1038/s43017-020-0040-3

Carbonneau, A. (1983). Méthodes de mesure simple de la surface foliaire exposée par hectare, élément déterminant du système de conduite de la vigne. OENO One, 17(4), 281. https://doi.org/10.20870/oeno-one.1983.17.4.1766

Chaves, M. M., Zarrouk, O., Francisco, R., Costa, J. M., Santos, T., Regalado, A. P., Rodrigues, M. L., & Lopes, C. M. (2010). Grapevine under deficit irrigation: Hints from physiological and molecular data. Annals of Botany, 105(5), 661–676. https://doi.org/10.1093/aob/mcq030

Cholet, C., Claverol, S., Claisse, O., Rabot, A., Osowsky, A., Dumot, V., Ferrari, G., & Gény, L. (2016). Tartaric acid pathways in Vitis vinifera L. (cv. Ugni blanc): A comparative study of two vintages with contrasted climatic conditions. BMC Plant Biology, 16(1), 144. https://doi.org/10.1186/s12870-016-0833-1

Deloire, A., Vaudour, E., Carey, V. A., Bonnardot, V., & van Leeuwen, C. (2005). Grapevine responses to terroir: A global approach. OENO One, 39(4), 149. https://doi.org/10.20870/oeno-one.2005.39.4.888

Diéguez, S. C., Lois, L. C., Gómez, E. F., & De La Peña, M. L. G. (2003). Aromatic composition of the Vitis vinifera grape Albariño. LWT - Food Science and Technology, 36(6), 585–590. https://doi.org/10.1016/S0023-6438(03)00064-1

Ferrer, M., González-Neves, G., Burgueño, J., Gabard, Z., & Camussi, G. (1997). Influencia de la intensidad de la poda y el raleo de racimos sobre la relación fuentefosa en Vitis vinifera L. Cv. Tannat. In Actas. XXII Congrès Mundial de La Vigne et Du Vin., Buenos Aires, Argentina.

Ferrer, M., Pereyra, G., Salvarrey, J., Arrillaga, L., & Fourment, M. (2020). 'Tannat' (Vitis vinifera L.) as a model of responses to climate variability. VITIS - Journal of Grapevine Research, 41-46 Pages. https://doi.org/10.5073/VITIS.2020.59.41-46

Fourment, M., & Piccardo, D. (2023). What grapes and wines to expect with the drought? Agrociencia Uruguay, 27(Suppl), e1206. https://doi.org/10.31285/AGRO.27.1206

Fourment, M., Bonnardot, V., Planchon, O., Ferrer, M., & Quénol, H. (2014). Circulation atmosphérique locale et impacts thermiques dans un vignoble côtier: Observations dans le sud de l'Uruguay. *Climatologie*, 11, 47–64. https://doi.org/10.4267/climatologie.589

Fourment, M., Ferrer, M., González-Neves, G., Barbeau, G., Bonnardot, V., & Quénol, H. (2017). Tannat grape composition responses to spatial variability of temperature in an Uruguay's coastal wine region. International Journal of Biometeorology, 61(9), 1617–1628. https://doi.org/10.1007/s00484-017-1340-2

Fourment, M., Tachini, R., Bonnardot, V., & Collins, C. (2024). Assessment of Albariño (Vitis vinifera sp.) plasticity to local climate in the Atlantic eastern coastal terroir of Uruguay: This article is published in cooperation with the XVth International Terroir Congress, 18-22 November 2024, Mendoza, Argentina. Guest editors: Federico Berli, Jorge Prieto and Martín Fanzone. OENO One, 58(4). https://doi.org/10.20870/oeno-one.2024.58.4.8196

Fraga, H. (2020). Climate Change: A New Challenge for the Winemaking Sector. Agronomy, 10(10), 1465. https://doi.org/10.3390/agronomy10101465

Glories, Y., & Agustin, M. (1992). Maturité phénolique du raisin, conséquences technologiques: Application aux millésimes 1991 et 1992. 56–61.

González-Neves, G., Charamelo, D., Balado, J., Barreiro, L., Bochicchio, R., Gatto, G., Gil, G., Tessore, A., Carbonneau, A., & Moutounet, M. (2004). Phenolic potential of Tannat, Cabernet-Sauvignon and Merlot grapes and their correspondence with wine composition. Analytica Chimica Acta, 513(1), 191–196. https://doi.org/10.1016/j.aca.2003.11.042

González-Neves, G., Ferrer, M., Gil, G., Charamelo, D., Balado, J., Barreiro, L., Bochicchio, R., Gatto, G., & Tessore, A. (2010). Estudio plurianual del potencial polifenólico de uvas Tannat en el sur de Uruguay. Agrociencia, 10–21. https://doi.org/10.31285/AGRO.14.622

Greer, D. H., & Weston, C. (2010). Heat stress affects flowering, berry growth, sugar accumulation and photosynthesis of Vitis vinifera cv. Semillon grapevines grown in a controlled environment. Functional Plant Biology, 37(3), 206–214. https://doi.org/10.1071/FP09209

Gutiérrez-Gamboa, G., & Fourment, M. (Eds). (2024). Latin American Viticulture Adaptation to Climate Change: Perspectives and Challenges of Viticulture Facing up Global Warming. Springer International Publishing. https://doi.org/10.1007/978-3-031-51325-1

Gutiérrez-Gamboa, G., Zheng, W., & Martínez De Toda, F. (2021). Current viticultural techniques to mitigate the effects of global warming on grape and wine quality: A comprehensive review. Food Research International, 139, 109946. https://doi.org/10.1016/j.foodres.2020.109946

Hailemichael, G., Catalina, A., González, M. R., & Martin, P. (2016). Relationships between Water Status, Leaf Chlorophyll Content and Photosynthetic Performance in Tempranillo Vineyards. South African Journal of Enology and Viticulture, 37(2). https://doi.org/10.21548/37-2-1004

Hochberg, U., Batushansky, A., Degu, A., Rachmilevitch, S., & Fait, A. (2015). Metabolic and Physiological Responses of Shiraz and Cabernet Sauvignon (Vitis vinifera L.) to Near Optimal Temperatures of 25 and 35 °C. International Journal of Molecular Sciences, 16(10), 24276–24294. https://doi.org/10.3390/ijms161024276

Horák, M., Balík, J., & Bieniasz, M. (2021). Effect of Leaf Area Size on the Main Composition in Grape Must of Three Varieties of Vitis vinifera L. in an Organic Vineyard. Sustainability, 13(23), 13298. https://doi.org/10.3390/su132313298

INAVI. (2025). Estaditicas de viñedos 2023. INAVI.

INUMET. (2020). Clasificación climática del Uruguay. https://www.inumet.gub.uy/clima/estadisticas-climatologicas/clasificacion-climatica

INUMET. (2023). Informe de Verano. Instituto Nacional de Meteorología.

INUMET. (2025a). Boletín Climático Marzo 2025. https://www.inumet.gub.uy/sites/default/files/2025-04/Boletin%20MARZO.pdf

INUMET. (2025b). Gráficas estadísticas pluviométricas [Data set]. https://www.inumet.gub.uy/clima/estadisticas-climatologicas/graficas-estadisticas-pluviometricas

IPCC. (2021). Reporte IPCC. https://www.ipcc.ch/report/ar6/wg1/

Jones, G. V., Reid, R., & Vilks, A. (2012). Climate, Grapes, and Wine: Structure and Suitability in a Variable and Changing Climate. In P. H. Dougherty (Ed.), The Geography of Wine (pp. 109–133). Springer Netherlands. https://doi.org/10.1007/978-94-007-0464-0_7

Kiaeian Moosavi, F., Cargnus, E., Pavan, F., & Zandigiacomo, P. (2018). Effects of grapevine bunch exposure to sunlight on berry surface temperature and Lobesia botrana (Lepidoptera: Tortricidae) egg laying, hatching and larval settlement. Agricultural and Forest Entomology, 20(3), 420–432. https://doi.org/10.1111/afe.12274

Le Roux, R., De Rességuier, L., Corpetti, T., Jégou, N., Madelin, M., van Leeuwen, C., & Quénol, H. (2017). Comparison of two fine scale spatial models for mapping temperatures inside winegrowing areas. Agricultural and Forest Meteorology, 247, 159–169. https://doi.org/10.1016/j.agrformet.2017.07.020

Mira De Orduña, R. (2010). Climate change associated effects on grape and wine quality and production. Food Research International, 43(7), 1844–1855. https://doi.org/10.1016/j.foodres.2010.05.001

Mori, K., Goto-Yamamoto, N., Kitayama, M., & Hashizume, K. (2007). Loss of anthocyanins in red-wine grape under high temperature. Journal of Experimental Botany, 58(8), 1935–1945. https://doi.org/10.1093/jxb/erm055

Mori, K., Sugaya, S., & Gemma, H. (2005). Decreased anthocyanin biosynthesis in grape berries grown under elevated night temperature condition. Scientia Horticulturae, 105(3), 319–330. https://doi.org/10.1016/j.scienta.2005.01.032

Natioanl Weather Services (NOAA). (2025). Cold & Warm Episodes by Season. https://origin.cpc.ncep.noaa.gov/products/analysis_monitoring/ensostuff/ONI_v5.php

Neethling, E., Barbeau, G., Coulon-Leroy, C., & Quénol, H. (2019). Spatial complexity and temporal dynamics in viticulture: A review of climate-driven scales. Agricultural and Forest Meteorology, 276–277, 107618. https://doi.org/10.1016/j.agrformet.2019.107618

OIV. (2009). Recueil des méthodes internationales d'analyse des vins et des moûts.

OIV. (2024). Base de datos [Computer software]. OIV. https://www.oiv.int/es

Pereyra, G., & Ferrer, M. (2024). New challenges for Uruguayan viticulture: Water management in the context of a changing climate. Agrociencia Uruguay, 27(NE2), e1195. https://doi.org/10.31285/AGRO.27.1195

Pillet, J., Berdeja, M., Guan, L., & Delrot, S. (2015). Berry response to water, light and heat stresses. In H. Gerós, M. M. Chaves, H. M. Gil, & S. Delrot (Eds), Grapevine in a Changing Environment (1st edn, pp. 223–257). Wiley. https://doi.org/10.1002/9781118735985.ch10

Pons, A., Allamy, L., Schüttler, A., Rauhut, D., Thibon, C., & Darriet, P. (2017). What is the expected impact of climate change on wine aroma compounds and their precursors in grape? OENO One, 51(2), 141. https://doi.org/10.20870/oeno-one.2016.0.0.1868

Quénol, H. (2014). Changement climatique et terroirs viticoles. Lavoisier Tec&doc.

Ravaz, M. (1911). L'effeuellage de la vigne. Annales d L'Ecole Nationale d'agriculture de Montpellier, 11, 216–244.

Sadras, V. O., Petrie, P. R., & Moran, M. A. (2013). Effects of elevated temperature in grapevine. II juice pH, titratable acidity and wine sensory attributes: Elevated temperature and wine sensory attributes. Australian Journal of Grape and Wine Research, 19(1), 107–115. https://doi.org/10.1111/ajgw.12001

Sánchez, L. A., & Dokoozlian, N. K. (2005). Bud Microclimate and Fruitfulness in Vitis vinifera L. American Journal of Enology and Viticulture, 56(4), 319–329. https://doi.org/10.5344/ajev.2005.56.4.319

Schultz, H. R., & Jones, G. V. (2010). Climate Induced Historic and Future Changes in Viticulture. Journal of Wine Research, 21(2–3), 137–145. https://doi.org/10.1080/09571264.2010.530098

Silva, A., Docampo, R., Camejo, C., & Barboza, C. (2018). Inventario de los suelos bajo viña del Uruguay. Principales características edafológicas de los viñedos uruguayos. INIA.

Tachini, R., Bonnardot, V., Ferrer, M., & Fourment, M. (2023). Topography interactions with the Atlantic Ocean and its impact on Vitis vinifera L. 'Tannat'. VITIS - Journal of Grapevine Research, 163-177 Pages. https://doi.org/10.5073/VITIS.2023.62.163-177

Tachini, R., Bonnardot, V., Quénol, H., & Fourment, M. (2026). Multi-scale climate analysis of two coastal wine terroirs in Uruguay: Adapting to climate change and heatwaves. Agricultural and Forest Meteorology, 378, 111000. https://doi.org/10.1016/j.agrformet.2025.111000

Tachini, R., Fourment, M., Bonnardot, V., Fanzone, M., & Ferrer, M. (2022). Study of mesoclimate and its impact on Vitis vinifera L. cv. Tannat in the Atlantic winegrowing region of Uruguay. 5 p.

Torregrosa, L., Bigard, A., Doligez, A., Lecourieux, D., Rienth, M., Luchaire, N., Pieri, P., Chatbanyong, R., Shahood, R., Farnos, M., Roux, C., Adiveze, A., Pillet, J., Sire, Y., Zumstein, E., Veyret, M., Le Cunff, L., Lecourieux, F., Saurin, N., … Romieu, C. (2017). Developmental, molecular and genetic studies on grapevine response to temperature open breeding strategies for adaptation to warming. OENO One, 51(2), 155. https://doi.org/10.20870/oeno-one.2016.0.0.1587

van Leeuwen, C., Sgubin, G., Bois, B., Ollat, N., Swingedouw, D., Zito, S., & Gambetta, G. A. (2024). Climate change impacts and adaptations of wine production. Nature Reviews Earth & Environment, 5(4), 258–275. https://doi.org/10.1038/s43017-024-00521-5

van Leeuwen, Destrac-Irvine, Dubernet, Duchêne, Gowdy, Marguerit, Pieri, Parker, De Rességuier, & Ollat. (2019). An Update on the Impact of Climate Change in Viticulture and Potential Adaptations. Agronomy, 9(9), 514. https://doi.org/10.3390/agronomy9090514

Verdenal, T., Dienes-Nagy, Á., Spangenberg, J. E., Zufferey, V., Spring, J.-L., Viret, O., Marin-Carbonne, J., & van Leeuwen, C. (2021). Understanding and managing nitrogen nutrition in grapevine: A review. OENO One, 55(1), 1–43. https://doi.org/10.20870/oeno-one.2021.55.1.3866

Vilanova, M., & Vilariño, F. (2006). Influence of geographic origin on aromatic descriptors of Spanish Albariño wine. Flavour and Fragrance Journal, 21(2), 373–378. https://doi.org/10.1002/ffj.1677